An Acad Bras Cienc (2020) 92(2): e20200796 DOI 10.1590/0001-3765202020200796
Anais da Academia Brasileira de Ciências | *Annals of the Brazilian Academy of Sciences*
Printed ISSN 0001-3765 I Online ISSN 1678-2690
www.scielo.br/aabc | www.fb.com/aabcjournal

CHEMICAL SCIENCES

An Overview on the Development of Electrochemical Capacitors and Batteries – Part I

VITOR L. MARTINS, HERBERT R. NEVES, IVONNE E. MONJE, MARINA M. LEITE, PAULO F.M. DE OLIVEIRA, RODOLFO M. ANTONIASSI, SUSANA CHAUQUE, WILLIAM G. MORAIS, EDUARDO C. MELO, THIAGO T. OBANA, BRENO L. SOUZA & ROBERTO M. TORRESI

Abstract: The Nobel Prize in Chemistry 2019 recognized the importance of Li-ion batteries and the revolution they allowed to happen during the past three decades. They are part of a broader class of electrochemical energy storage devices, which are employed where electrical energy is needed on demand and so, the electrochemical energy is converted into electrical energy as required by the application. This opens a variety of possibilities on the utilization of energy storage devices, beyond the well-known mobile applications, assisting on the decarbonization of energy production and distribution. In this series of reviews in two parts, two main types of energy storage devices will be explored: electrochemical capacitors (part I) and rechargeable batteries (part II). More specifically, we will discuss about the materials used in each type of device, their main role in the energy storage process, their advantages and drawbacks and, especially, strategies to improve their performance. In the present part, electrochemical capacitors will be addressed. Their fundamental difference to batteries is explained considering the process at the electrode/electrolyte surface and the impact in performance. Materials used in electrochemical capacitors, including double layer capacitors and pseudocapacitive materials will be reviewed, highlighting the importance of electrolytes. As an important part of these strategies, synthetic routes for the production of nanoparticles will also be approached (part I).

Key words: rechargeable batteries, electrochemical capacitors, electrochemical energy storage, material for batteries, materials for electrochemical capacitors.

INTRODUCTION

In 2019, the Nobel Prize in Chemistry was awarded to Goodenough, Whittingham and Yoshino for the development of Li-ion batteries. Their findings paved the way for the electric revolution in which we live today. From devices that enabled information access nearly everywhere to electric vehicles, they are all powered by a Li-ion battery. Moreover, the use of electrochemical energy storage devices in the power supply grid is on the rise, enabling power production to be more concentrated in intermittent renewable sources. Their works were developed during the 1980s and early 1990s, but obviously the technology kept improving over the years, and materials that can store more energy density have been described over the last decades. This is because there is a need for devices that can deliver energy for either a longer time (high energy density) or faster (high power density).

For instance, electrochemical capacitors are another class of electrochemical energy storage device, but, unlike batteries, they

normally show low energy density yet high power. These differences in performance arise from the different electrochemical process that takes place during cell charge and discharge. In a typical double-layer capacitor, the only process occurring is the charge and discharge of the electric double-layer (interface between electrode and electrolyte), which is a fast process. The charge of the double-layer involves the charge compensation generated at the electrode surface by the ions in solution, this generated charge at the electrode surface comes from an external source, *ie.* when the device is plugged to the socket and it is being charged. The double-layer charging is a physical process (movements of ions and electrons) and it results in a high-power event (the process is fast, and it can deliver – or store – the energy quickly), but, since it is limited to the material surface area only, also results in low energy density (it cannot operate for much long). On the other hand, batteries show faradaic reactions, therefore, there is change on oxidation state of active materials during charge and discharge, which can happen in the bulk material as well as the surface, resulting in high energy. However, it depends on the slow kinetics of these faradaic reactions, resulting in low power. In between the materials for batteries and double-layer capacitors, there are the pseudocapacitive materials, which rely on fast faradaic reactions, mimicking a capacitor. These fast faradaic reactions occurs at the electrode surface. Figure 1 shows the relationship between energy and power density, the so-called Ragone plot, for various energy storage systems from electrostatic capacitors (physical) to combustion engines (chemical). The electrochemical systems need to be improved to gain more energy and power so they can compete with combustion engines, especially for transport applications. This review will show different strategies that have been used to build devices that can show such requirements.

ELECTROCHEMICAL CAPACITORS

Electrochemical capacitors show higher power and lower energy density when compared to batteries because the electrochemical processes involved in charge storage are different. These processes can vary even among electrochemical capacitors. Figure 2 compares an electrostatic capacitor (or physical capacitor), a double-layer capacitor, and a pseudocapacitive material-based capacitor (polyaniline (PANI), as example). In this section, the former two kinds of capacitors will be reviewed, focusing on the electrochemical processes and strategies to improve these devices.

Electrochemical double-layer capacitor

As mentioned above, electrochemical double-layer capacitors (EDLCs) rely on the physical interaction between the electrode surface and ions present in the electrolyte. This interaction is known as the electric double-layer. As one electrode is polarized positively, anions will migrate within the solution to locally compensate the positive charge, whereas the other electrode is polarized negatively, and therefore, cations will migrate to this negative surface to compensate

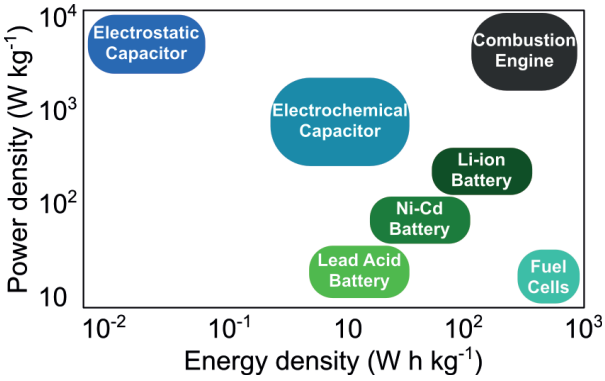

Figure 1. Ragone plot showing energy and power density for different energy storage systems.

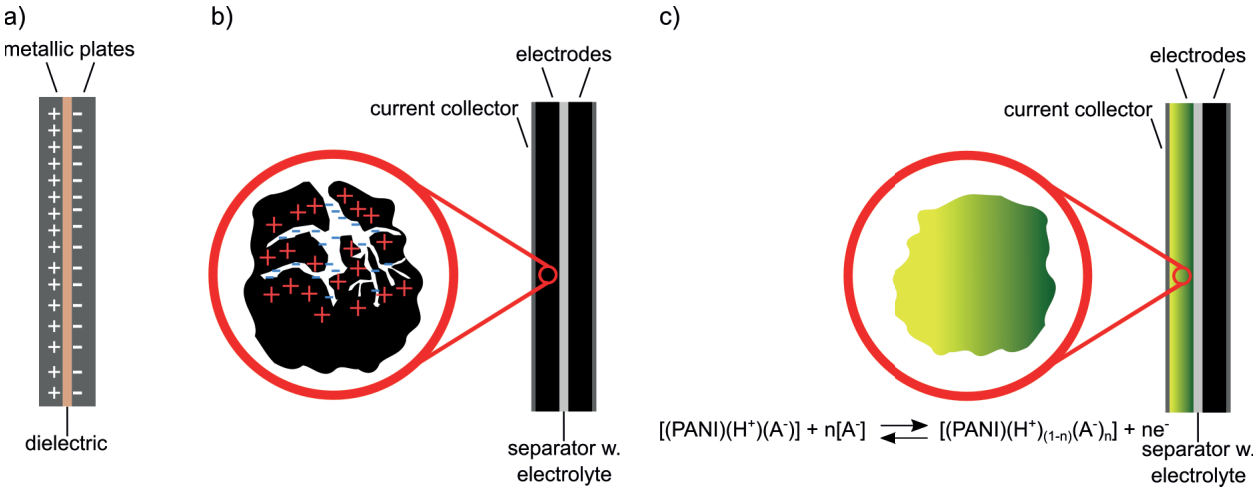

Figure 2. (a) electrostatic capacitor, (b) electrochemical double-layer capacitor, and (c) electrochemical capacitor with pseudocapacitive material (PANI as example).

the charge. Each electrode has a double-layer, one being deficient and another having excess of electrons, which in turn will result in a double-layer containing mostly anions and cations, respectively. The formation of both double-layers is concomitant and requires a current flow between both electrodes, which is the capacitor charge process. This process occurs until the cell voltage reaches the maximum determined cell voltage. Once the EDLC is charged, the double-layer is maintained and the stored energy can be used afterwards. While the EDLC is used, *ie.* the capacitor discharge process, a current will flow on the opposite direction, and both double-layers will start to be undone. Once the device is completely discharged, cell voltage will be zero.

Electrodes

The capacitance (C) of a capacitor can be calculated from equation (1):

$$C = \frac{\varepsilon_0 \varepsilon_r A}{d} \quad (1)$$

where ε_0 and ε_r are the electric constant and the dielectric constant between charge separation, respectively; A is the electrode surface area; and d is the separation of two plates in a physical capacitor, or the thickness of the double-layer in the EDLC. There are two main reasons for EDLCs to present much higher capacitance than a physical capacitor, that can be observed from equation (1). Firstly, the thickness of double-layer is several orders of magnitudes smaller than the separation between two plates in a physical capacitor, and secondly, the surface area achieved using carbonaceous materials is in order of a couple of thousands m^2 per gram. Therefore, activated carbon (AC) and other carbonaceous materials with high surface area are the most employed in EDLC development.

AC is produced from many precursors, but most of commercially available ACs are prepared from coconut shell (Hall et al. 2010). AC preparation involves basically two steps. The first is the carbonization of a precursor at high temperatures, which can be made under an oxygen-free atmosphere or by hydrothermal treatment (Wang et al. 2018). Then, the charcoal-like product is activated, also at high temperature, either through a mixture of inert and oxidizing atmospheres or through chemical oxidation. Different processes lead to different textural properties, varying pore size distribution, surface area, and possibly chemical functionalization.

These different properties will have an impact on capacitance. Not only changing the surface area will change the capacitance, but pore size can facilitate or hinder mass transport (Chmiola et al. 2008, Jäckel et al. 2016, Sillars et al. 2011), while chemical functionalization can increase interactions between ions and electrode surface, increasing the specific capacitance (Abbas et al. 2019). For instance, it is believed that nitrogen functionalization increases the AC specific capacitance through faradaic reactions, behaving as a pseudocapacitive material (Candelaria et al. 2012). However, even with the increment in capacitance, it has been difficult to determine the exactly role of functionalization and different pore size distribution (Simon & Gogotsi 2008).

As mentioned above, many precursors have been used for AC preparation. It is worth mentioning that carbonization of biomass has attracted great attention of many research groups (Titirici et al. 2015, Wu et al. 2013, 2016), due to the interest in adding value to biomass that would be treated as waste instead.

An obvious alternative to AC is the employment of graphene or graphene-like materials. Graphene is known to have a large surface area, comparable to AC, and, as a 2D material, this area could be doubled if accessible by the electrolyte in both sides. However, due to layer stacking during processability and electrode manufacturing, the achieved capacitance is below expectations and it is outperformed by AC (Béguin et al. 2014). A few strategies have overcome this problem, for instance, vertically aligned graphene can be growth directly onto Ni current collector, making use of both sides of the layer, resulting in a greater capacitance (Cai et al. 2014, Miller & Outlaw 2015). Changing the graphene textural properties is also an alternative to increase surface area (Kholmanov et al. 2013, Lopes et al. 2018, Salvatierra et al. 2013), and therefore the specific capacitance. This change can be done through activation of graphene with similar procedures described above (Zhang et al. 2014).

Electrolytes

An EDLC electrolyte holds the ions that interact with the electrodes. Positive and negative electrodes usually interact with anions and cations, respectively, to form two electrical double-layers. Therefore, the ions need to have good mobility for a fast charge-discharge mechanism, which means that the electrolyte must have a high ionic conductivity.

Electrolytes can be classified by the solvent used in their formulation, and each of them has advantages and disadvantages when compared. The most common types are water, organic solvents, and ionic liquids (ILs). There are three main properties that have the most impact: viscosity, dielectric constant, and electrochemical stability. Each of these factors have a practical impact on the EDLC performance and metrics. Viscosity has great impact on ionic conductivity and capacitance itself. Firstly, as more viscous is the liquid, less mobility the ions possess, decreasing ionic conductivity, which in turn penalize the device power density. Secondly, the activated carbon micropores can be difficult to access when too viscous electrolytes are used, due to the low wettability of electrode/electrolyte. Moreover, the dielectric constant of the electrolyte solvent is directly proportional to the electrode capacitance, as shown in Equation 1, and normally the dielectric constant is higher for polar than for nonpolar solvents. However, polar solvents usually presents higher viscosities and possibly lower electrochemical stability, especially for polar protic solvents (Conway 1999). In addition, the electrochemical stability can depend on other

aspects of the solvent, for instance, molecules with conjugated double bonds normally show a diminished electrochemical stability. The added salt can also play an important role in the electrochemical stability, since cations and anions can be reduced or oxidized at too high polarization. From equation (2) it is possible to see how important it is to have a high operating voltage, ie. high electrochemical stability of the whole system electrodes/electrolyte, to obtain a high energy density EDLC:

$$E = \frac{CV^2}{2} \quad (2)$$

where E, C and V are energy density (W h g^{-1}), capacitance (F g^{-1}), and operating voltage (V). For instance, increasing the operating voltage from 1 to 3 V results in an increment of 9 times in energy density.

Moreover, the ion size impacts on the electric double-layer and then on the obtained capacitance, since the relationship between ion size and pore size distribution plays a major role in the final capacitance, due to pore accessibility. Therefore, choosing the appropriate salt to the electrolyte requires one to consider the pore distribution of the activated carbon used in the electrode formulation.

Aqueous electrolyte can be acidic, alkaline or neutral water solutions. The issue with acidic and alkaline solutions is that the former will have a lower negative voltage limit due to the presence of H^+ and the H_2 evolution, and the latter will show lower positive voltage limit due to the presence of OH^- and the O_2 evolution. Overall, both of them will have a limited electrochemical stability which will decrease the EDLC energy density, as shown in Equation 2. On the other hand, the ionic conductivity of these electrolytes is high, guarantying a superior power density due to elevated ion mobility. Neutral aqueous solutions can present higher electrochemical stability but lower ionic conductivity than the others aqueous electrolyte counterpart. For instance, Fic et al. (2019) reported that an EDLC with aqueous solution of 1 mol L^{-1} Li_2SO_4 can show an operating voltage up to 1.6 V, but they also showed that the cell internal pressure starts to increase when cell voltage exceeds 1.2 V, clearly indicating that cell optimization can be carried out to enhance operating voltage and mitigate electrolyte decomposition. For comparison, aqueous electrolyte containing KOH, H_2SO_4 or Li_2SO_4 show ionic conductivities of 540, 750 and 70 mS cm^{-1}, respectively, while the first two show operating voltages of *ca.* 0.8 V, while the last one could go up to 1.6, as mentioned above (Fic et al. 2019, Ramachandran & Wang 2018).

To enhance the operating voltage, aprotic organic solvents can be used in the electrolyte formulation. The state-of-the-art regarding organic solvent electrolyte contains propylene carbonate (ε_r = 66, at 20 °C) or acetonitrile (ε_r = 36, at 20 °C), and considering that the latter has a flash point of 6 °C ($T_{boiling}$ = 82 °C) against 132 °C ($T_{boiling}$ = 242 °C) for the latter, the most common used between both is propylene carbonate (Gagliardi et al. 2007, Simeral & Amey 1970). The salt added in both is tetraethylammonium tetrafluoroborate ($TEABF_4$), normally at 1 mol L^{-1} (Béguin et al. 2014). Other salts are also investigated, as $LiBF_4$ and tetramethylammonium ($TMABF_4$), which present smaller cations, so the electric double-layer could host more cations and then increase capacitance. However, the solubility of these salts is lower than $TEABF_4$ (Nambu et al. 2013). Another strategy is changing the anion BF_4^- for bis(oxalato)borate or difluoro(oxalato)borate, increasing the solubility of the TMA^+ salt in propylene carbonate (PC) (Nanbu et al. 2006a, b, 2007).

Schütter et al. (2015, 2016) have proposed computational screening of solvents for electrolyte production. They scrutinized organic compounds considering several

properties, as flash point and melting temperatures, viscosity, solubility of salts and electrochemical stability, and, on top of that, they considered only commercially available compounds. First, they correlated their method by using nitrile compounds as glutaronitrile, 2-methylglutaronitrile and adiponitrile. They concluded that the computational screening was successful on selecting appropriate compounds to be used as solvent for EDLC electrolytes (Schütter et al. 2015). Later, they widened the compounds class and selected the 3-cyano-propionic acid methyl ester. The electrolyte containing the selected solvent and $TEABF_4$ showed an operating voltage of 3.5 V and long-term stability (Schütter et al. 2016).

Another class of electrolyte that has received great attention is IL. ILs are salts that are liquid at room temperature. As they are composed only by ions, they show intrinsic ionic conductivity; in addition, they also show high thermal stability and wide electrochemical window (Eftekhari 2017, MacFarlane et al. 2016, Salanne 2017). There is a myriad of possible ILs since they can be produced by the appropriate matching of many cations and anions. Common cation classes are imidazolium ($Im_{x,y,z}^+$), pyrrolidinium ($Pyr_{x,y}^+$), piperidinium ($Pip_{x,y}^+$) and other tetraalkylammoniuns ($N_{x,y,z,w}^+$), phosphoniuns ($P_{x,y,z,w}^+$), sulfoniuns ($S_{x,y,z}^+$) among others – *x,y,z,w* indicates length of alkyl chain. On the other hand, common anions are bis(trifluoromethylsulfonyl) imide (Tf_2N^-), bis(fluorosulfonyl)imide (FSI^-), hexafluorophosphate (PF_6^-), tetrafluoroborate (BF_4^-), and many more (MacFarlane et al. 2016, Martins & Torresi 2018, Torresi et al. 2018). Ions can be tailored by functional groups for specific tasks, which increases the number of possible ILs (Monteiro et al. 2008, 2010). The electrochemical stability of ILs is normally evaluated using inert electrodes like glassy carbon, however, when utilized as EDLC electrolyte, the stability of the current collector and the electrode (AC, binder and carbon black) must be taken into consideration, and an appropriate technique for maximum operation voltage determination must be done (Martins et al. 2018b, Weingarth et al. 2013).

Two ILs have been mostly used and can be considered the benchmark when comparing new liquids: 1-ethyl-3-methyl imidazolium BF_4 ($[Im_{1,2}][BF_4]$) and *N*-butyl-*N*-methyl pyrrolidinium Tf_2N ($[Pyr_{1,4}][Tf_2N]$), achieving 3.8 and 3.7 V, respectively, depending on binder and AC (Martins et al. 2018a, b, Weingarth et al. 2013). A polymeric binder has shown to have a great impact on the operating voltage, increasing from 2.7 to 3.8 V using the same IL $[Im_{1,2}][BF_4]$ (Martins et al. 2018b). Moreover, the use of a polymeric IL as binder in electrode preparation can increase the operating voltage and also the capacitance, being a promising alternative to inert binders (Martins et al. 2017b).

Different cations combined with Tf_2N^- were also reported. The addition of an ether chain in a phosphonium cation remarkably increased the capacitance when compared with an analog cation with an alkyl chain, due to increased mobility of the ether chain (Rennie et al. 2013). 1-(Pentamethylbenzyl)azepanium ($Azp_{x,y}^+$) was also suggested as a promising cation to be applied in EDLC, since it is an industrial by-product. It showed competitive operating voltage and capacitance compared to $[Pyr_{1,4}][Tf_2N]$, but tests were carried out at 60 °C due to its high melting temperature (Pohlmann et al. 2015). ILs with sulfonium cations showed elevated capacitance, probably due to smaller cation size than $Pyr_{1,4}^+$ but lower maximum operating voltage, penalizing the EDLC energy density (Rennie et al. 2015).

All the anions cited above have fluorine in their composition, and one of the focus has been to find fluorine-free anions that still

have competitive electrochemical properties. Dicyanamide($N(CN)_2^-$) is one of the most promising fluorine-free anions, as ILs containing this anion show ionic conductivity similar to the state-of-the-art electrolyte. For instance, $[Pyr_{1,4}][N(CN)_2]$ shows 12.0 mS cm^{-1} against the 12.2 mS cm^{-1} of 1 mol L^{-1} $TEABF_4$ in PC (Hall et al. 2010, MacFarlane et al. 2002). However, these ILs suffer from low electrochemical stability, but even operating at 2.6 V, their EDLC shows similar energy density than an EDLC containing the Tf_2N^- counterpart at 3.5 V (Wolff et al. 2015). ILs containing the anion tricyanomethanide ($C(CN)_3^-$) show the same trend, while ionic conductivity can be 9.4 mS cm^{-1} for $[Im_{1,4}][[C(CN)_3]$, their normally have low operating voltage and overcome the energy density of EDLC with $[Pyr_{1,4}][Tf_2N]$ operating at low power (Martins et al. 2017a). On the other hand, the anion tetracyanoborate ($B(CN)_4^-$) also shows relatively high conductivity while keeping a wide electrochemical stability. EDLC containing the IL $[Pyr_{1,4}][B(CN)_4]$ can operate up to 3.7 V and outperform the energy density of the EDLC using a Tf_2N^- analogue at all tested power densities (Martins et al. 2018a). It is worth mentioning that strategies such as mixing different ILs to tailor the electric double-layer has also been considered and more symmetrical charge distribution between both electrodes has been observed (Van Aken et al. 2015).

Solid electrolytes, or gel polymer electrolytes, have also been considered for EDLCs. They have the advantage of being safer, since there is no possibility of leakage, and more importantly they are normally nonflammable. Mixture of poly(ethylene oxide) with different salts is the most common solid electrolyte, but other mixtures have been proposed, including the use of poly IL (Ayalneh Tiruye et al. 2015, Kim et al. 2013, Pont et al. 2009). The bottleneck of solid electrolytes is the low ion mobility, which results in low ionic conductivity compared to liquid electrolytes, hampering the device power density (Xue et al. 2015).

Pseudocapacitive materials

There is an effort to enable electrochemical capacitors with higher energy and power densities to go beyond the employment of electrodes based on carbon-derived materials (Lin et al. 2018b). Such goal can be achieved by the use of the so-called pseudocapacitive materials. These materials, differently from the carbonaceous ones, do not retain charge exclusively from ion adsorption at the electrode/electrolyte interface, but from reversible and fast redox reactions near or at the electrode material surface (Augustyn et al. 2014, Conway 1999). These sorts of electrochemical processes, despite their faradaic nature, exhibit capacitive features, such as a rectangular-shaped potentiodynamic profile and almost linear galvanostatic charge-discharge curves. For that reason, those phenomena are called pseudocapacitive (from greek: *pseudos*, pretended and not real) (Conway 1999, Brousse et al. 2017). Traditionally, according to Conway (Conway 1999, Conway et al. 1997), several faradaic mechanisms can result in capacitive electrochemical features: (1) intercalation pseudocapacitance, (2) underpotential deposition (3) redox pseudocapacitance or specific adsorption with charge transfer, and (4) charge compensation in conducting polymers.

These four processes have different physical natures and can occur in plenty of materials, revealing, however, the same electrochemical behavior. Intercalation pseudocapacitance, for instance, takes place when ions intercalate (due to charge transfer) into the active sites of redox materials through tunnel or channels, without crystallographic phase change (Augustyn et al. 2014, Jiang & Liu 2019). Underpotential deposition, on the other hand, occurs when depositing a metal ion on a different metal

surface, above its redox potential, forming a monolayer or submonolayer of deposited metal. One straightforward example is the deposition of Pb^{2+} onto Au surface (Chen et al. 1993). Besides, redox pseudocapacitance arises during the adsorption of ions at the electrode surface concomitantly with partial charge transfer, due to specific interactions between the ion's valence electrons and the electrode's surface orbitals, like in a Lewis acid-base donor-acceptor interaction (Conway 1991). It is worth to mention, as an example, the adsorption of H^+ into $Ru_2O.nH_2O$ surface (Ardizzone et al. 1990). The latter pseudocapacitive process listed here appears during the electrochemical oxidation/reduction of conducting polymers. As long as polymeric chains are being oxidized/reduced, ions from the electrolyte are incorporated in the polymer backbone, in order to compensate the generated charges. All those mechanisms are schematized in Figure 3.

As mentioned before, those processes arise from different physical natures, but the materials display the same electrochemical features. Such singularity is due to the relationship between the electrical potential and the extent of charge developed at the electrode surface as a result of interfacial phenomena or along the so-called inner surface of materials (Ardizzone et al. 1990). The following expression was proposed by Conway (1999) and Conway et al. (1997):

$$E \sim E^o - \frac{RT}{nF}\ln\left(\frac{X}{1-X}\right) \quad (3)$$

wherein E is the electrode potential, R is the real gas constant, n is the number of electrons, F is the Faraday constant, T is the temperature and X is the fractional coverage, which varies for each type of pseudocapacitive process. Besides such a thermodynamic approach, pseudocapacitive materials hold the promise for better electrochemical capacitors materials, due to their kinetic behavior. The energy storage in such materials is limited to reactions that occur at electrode surface or are limited to surface availability, differently from solid-state diffusion (as battery materials), displaying high rate capability (Augustyn et al. 2014). There is a significant difference between transition metal oxides that display a pseudocapacitive behavior and those that do not. The latter are employed as battery materials. However, some of such battery-type transition metal oxides, when nanostructured from bulk to a few nanoscale dimensions, display a capacitive electrochemical signature, as shown in Figure 4 (Okubo et al. 2007). This is because, as pointed out, pseudocapacitive processes are surface dependent. The increase in surface area via nanostructuration increases the availability of redox sites at the surface, promoting the so-called "surface redox processes" (in contrast with "bulk redox processes"). Such nanostructuration, also suppresses phase transformation of some battery-type materials to a large extent and stimulate high-rate capability due to the shortening of diffusion pathway length. All those factors give raise to capacitive electrochemical signatures, despite their redox nature. Such kind of pseudocapacitive behavior was classified by Dunn (Augustyn et al. 2014) as extrinsic pseudocapacitance. In comparison with pseudocapacitance present in bulk materials such as RuO_2 and MnO_2, *ie.* intrinsic pseudocapacitance. The features concerning pseudocapacitive materials and battery-type ones and their frontiers rendered plenty of discussions, which is the topic of others reviews (Augustyn et al. 2014, González et al. 2016, Jiang & Liu 2019).

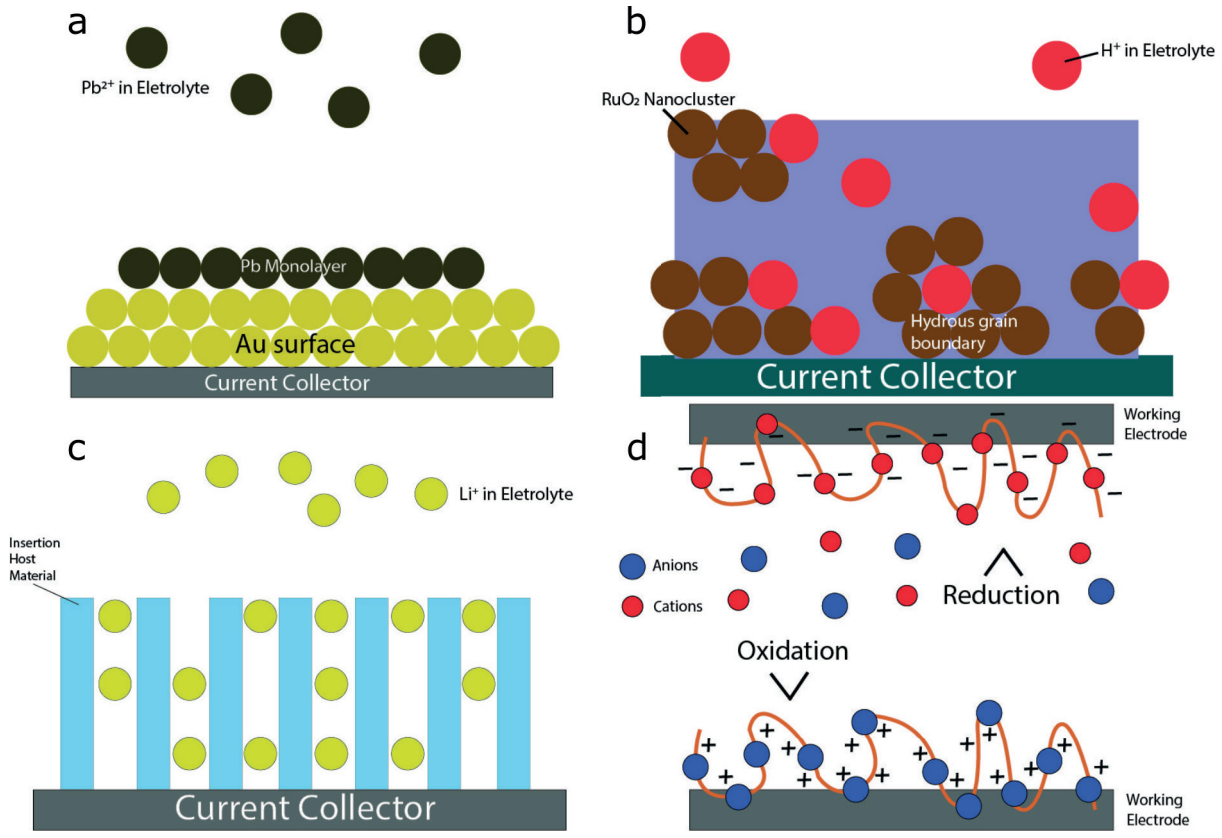

Figure 3. General scheme of pseudocapacitive process: a) underpotential deposition of Pb^{2+} onto Au b) redox pseudocapacitance C) intercalation pseducapacitance of Li^{+} into layered metal oxide d) charge compensation process (doping) of conducting polymers.

Electrodes

Metal oxides

Transition metal oxides (TMOs) are considered promising electrode materials for high energy and high power density electrochemical capacitors, as they possess expressive specific capacitance despite suffering from low electronic conductivity (Beguin & Frackowiak 2013). The main TMOs studied for electrochemical capacitor applications are RuO_2, MnO_2, the so-called MXene materials and oxides with spinel structure such Mn_3O_4, Fe_3O_4 and $MnFe_2O_4$ (Augustyn et al. 2014, Jiang & Liu 2019, Lin et al. 2018a).

RuO_2 was one of the earliest pseudocapacitve materials reported. It presents high specific capacitance (over 700 F g^{-1}) (Augustyn et al. 2014), large potential window, high proton conductivity, high rate capability, and metallic type electronic conductivity. Also, the hydrated state of the oxide and its crystallography have influence over RuO_2 pseudocapacitance behavior and specific capacitance values. Moreover, for electrogenerated material, factors like surface treatment of obtained films, such as annealing and anodization, and deposition potential range seem to play a considerable role at RuO_2 pseudocapacitive behavior (Ahn et al. 2006, Patake et al. 2009). Nevertheless, the high cost of such material, its toxicity and scarcity still limit its practical application as electrode material. However, MnO_2 arises as a cheaper and more environmentally friendly electrode material. Its pseudocapacitive behavior was

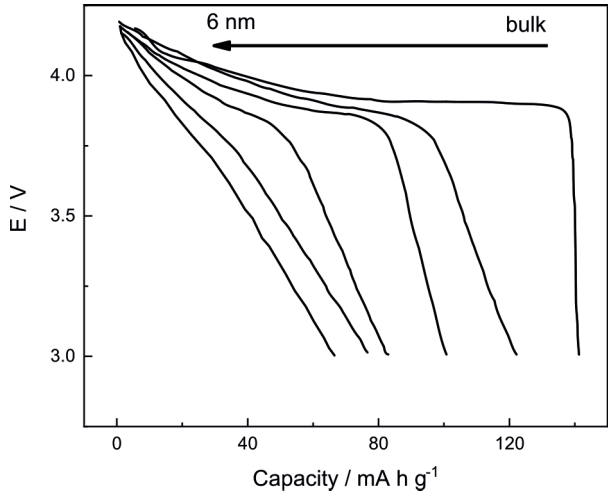

Figure 4. Particle size effect on the voltage profile during galvanostatic reduction of $LiCoO_2$. Adapted from (Okubo et al. 2007) with permission from the American Chemical Society.

first reported by Lee & Goodenough (1999) for amorphous $MnO_2{\cdot}nH_2O$ in KCl aqueous media. Capacitance values near 200 F g^{-1} were recorded, despite its theoretical specific capacitance near 1233 F g^{-1} (assuming a potential window ~0,9 V, for one-electron transfer). Such difference stems from MnO_2 poor electronic conductivity (10^{-5} to 10^{-6} S cm^{-1} (Zhao et al. 2017)), limiting the charge storage to a thick layer of surface. However, in the form of thin or ultrathin films, specific capacitances over 1000 F g^{-1} were achieved (Toupin et al. 2004). Several attempts were made in order to enlarge such conductivity and specific capacitance values, such as changing the crystallographic structure, using different synthetic pathways, doping with metal ions (Augustyn et al. 2014, Wang et al. 2012) and reactants media pH (Kandalkar et al. 2010). Also, for electrogenerated ones, the addition of some ligands to electrodeposition bath favored the formation of composites with carbon, enhancing electronic conductivity (Jiang & Kucernak 2002).

Spinel transition metal oxides, like Fe_2O_3, Mn_3O_4 and Co_3O_4 (Augustyn et al. 2014) together with mixed spinel transition metal oxides such as $MnFe_2O_4$ (Kuo & Wu 2006) and $NiCo_2O_4$ (Yu et al. 2013) are interesting materials due to their robust crystalline architecture with three dimensional diffusion pathways (Augustyn et al. 2014, Chen et al. 2015, Lin et al. 2018a). Among them, the Fe_2O_3, $MnFe_2O_4$ and Mn_3O_4 show the typical pseudocapacitive electrochemical features, mostly the rectangular shaped potentiodynamic profile, in aqueous media. Also, like MnO_2, Mn_3O_4 shows poor electronic conductivity and, as a consequence, only very thin coatings should be employed. For instance, 1.2 µm thick electrode based on Mn_3O_4 nanoparticles displayed a maximum specific capacitance value of 314 F g^{-1} (Dubal et al. 2010), in comparison with other electrodes based on different kinds of Mn_3O_4 whose specific capacitance values lies in the range of 100 – 200 F g^{-1} (Lee et al. 2012). On the other hand, $MnFe_2O_4$ and Fe_2O_3 shown no expressive improvements with nanostructering, their specific capacitance for chemical and electrochemical electrodes remains in the modest range of 100 – 150 F g^{-1} (Brousse et al. 2017). Also, their pseudocapacitive mechanism remains unraveled (Augustyn et al. 2014). Differently from others spinel materials, Co_3O_4 and $NiCo_2O_4$ can act as battery-type materials, due to the formation of oxyhydroxides along the charge storage process in alkaline media, which gives higher capacitance values in comparison with others spinel-type metal oxides. However, during galvanostatic charge-discharge processes, in some cases, small plateaus corresponding to purely faradaic reactions are observed, instead of capacitor-like triangular profile (Yuan et al. 2013). Aside, some cobalt oxides obtained by successive ionic layer adsorption and reaction revealed reasonable pseudocapacitive properties (Kandalkar et al. 2008).

The majority of electrodes based on such materials are studied in aqueous electrolytes

(Brousse et al. 2017). However, the efforts to push towards pseudocapacitive-material-based devices lead to the use of non-aqueous electrolyte. Most of them are based on non-aqueous lithium-ion or sodium-ion electrolytes. In such media some transition metal oxides exhibit intercalation pseudocapacitance due to the intercalation of Na^+ or Li^+ ions. Also, the electrolyte enables capacitance over a wider potential range in comparison with aqueous media, and therefore higher energy densities (Augustyn et al. 2014). As electrode active material for that kind of pseudocapacitance, it is worth mentioning orthorhombic Nb_2O_5 (T-Nb_2O_5) (Lin et al. 2018a). The energy storage properties of Nb_2O_5 is known since 1980 (Ohzuku et al. 1987), however, only the pseudocapacitive properties of T-Nb_2O_5 has been shown more expressively. Due to the redox couple Nb^{+5}/ Nb^{+4}, charge storage occurs upon 2 Li^+ per Nb_2O_5 with capacity over 720 C g^{-1} (Ohzuku et al. 1987). Moreover, the crystallinity strongly affects the pseudocapacitive properties of such Nb_2O_5 (Kim et al. 2012). While an amorphous Nb_2O_5 displays the lower capacitance of 262 F g^{-1} (4 min. charge-discharge curve), a T-Nb_2O_5 shows 555 F g^{-1} (4 min. charge-discharge curves), in spite of the higher surface area of the amorphous oxide. However, like other transition metal oxides, it lacks reasonable electronic conductivity, demanding their use as thin or ultrathin films and the addition of conductive compounds, hampering their application in practical devices (Lin et al. 2018a).

The seek for high-performance pseudocapacitive materials leads to the development of various other metal oxides with a myriad of structural features and compositions being the subject of others reviews (González et al. 2016, Hall et al. 2010, Kumar et al. 2018)

MXenes

MXenes are 2D transition metal carbides, nitrides and carbonitrides obtained by the selective chemical etching of A element layers in an MAX structure, where "M" is an early transition metal oxide (such as Sc, Ti, Zr,Hf, V,Nb,Ta,Cr,Mo, etc.), "A" is an A group element, mainly group A-13 and A-14 (such as Al, Si, S, Ga, Ge, As, Cd, In, Sn etc.) and "X" is carbon/nitrogen (Naguib et al. 2012). In general, the MAX phase is stable, however, the relative weakness of the M-A bound in comparison with the M-X bond allows etching by treatment with HF (Naguib et al. 2011). Also, the method enables functionalization of MXene with -F or -OH, influencing the physicochemical properties of obtained materials (Alhabeb et al. 2017a). In terms of pseudocapacitive materials, $Ti_3C_2T_x$ (T_x = OH / F) is undoubtedly the most studied MXene, being obtained by selective etching of an Al layer in Ti_3AlC_2 phase.

Most MXenes are studied in aqueous electrolytes. In the case of $Ti_3C_2T_x$ (Ghidiu et al. 2014, Lukatskaya et al. 2013, Naguib et al. 2012), it is known that its pseudocapacitance is related to Ti redox changes accompanied by cation intercalation (Lin et al. 2018a). Interestingly, some cations readily intercalate into $Ti_3C_2T_x$ by only immersing it in a suitable cation solution (Lukatskaya et al. 2013). Also, some promising results are observed for free standing clay-type $Ti_3C_2T_x$ paper electrode *e.g* a volumetric capacitance exceeding 900 F cm^{-3}, in H_2SO_4 electrolyte (Ghidiu et al. 2014). Also, still employing paper electrode, a range of 300 – 400 F cm^{-3} is observed in neutral media (Lukatskaya et al. 2013). However, despite those values, the narrow potential window allowed by aqueous media hinders the widespread use of MXene based electrochemical capacitors.

Polymers

Pseudocapacitance in conducting polymers arises from their redox reactions, which are followed by entrapment of electrolyte ions at the polymer's backbone in order to compensate the generated charges, which is often called doping process. Conducting polymers usually display higher specific capacitance values in comparison with some transition metal oxides (Muzaffar et al. 2019), relative low cost and can be readily synthetized chemically or electrochemically (González et al. 2016, Huguenin & Torresi 2008). However, conducting polymer-based electrodes present lower cyclability (Beguin & Frackowiak 2013, González et al. 2016) and conductivity loss, due to polymer swelling and shrinking along innumerous cycles (Beguin & Frackowiak 2013). The most common employed conducting polymers are PANI (Banerjee et al. 2019, Karami et al. 2003, Neves & Polo Fonseca, 2002, Ryu et al. 2002), polypyrrole (PPy) (Fan & Maier 2006, Snook et al. 2004, Wang et al. 2007), polythiofene (PTh) (and its derivates) (Snook et al. 2011, Villers et al. 2003), and poly(3,4-ethylenedioxythiophene) (PEDOT) (Her et al. 2006, Snook et al. 2011, Villers et al. 2003). Each of them shows electroactivity in various potential ranges, depending on the electrolyte (organic and aqueous) (Maia et al. 1996, Varela et al. 2001). It is important to point out that the electrolyte displays a great importance over charge compensation in conducting polymers. Such influence was deeply explored for polymers like PPy (Maia et al. 1996, Peres et al. 1992, Torresi et al. 1995), PANI (De Albuquerque Maranhão & Torresi 1999a, b, Torresi et al. 1993) and PEDOT (Lé et al. 2019) by means of *in situ* electrochemical techniques such as electrochemical crystal quartz microbalance (De Albuquerque Maranhão & Torresi 1999a, 1999b, Lé et al. 2019, Maia et al. 1996, Peres et al. 1992, Torresi et al. 1993, 1995) and optical beam deflection (Matencio et al. 1995). In general, the specific capacitance of chemically synthetized conducting polymer-based electrode ranges from 100 to 600 F g^{-1}, depending on the media. For organic electrolytes , values below 300 F g^{-1} are usually observed (Laforgue et al. 2002, Soudan et al. 2001, Villers et al. 2003). In order to circumvent problems regarding volumetric changes, composite materials such as polymer-ceramic, polymer-metal, polymer-carbon (Lin et al. 2018a) are being employed. One strategy to improve the conducting polymer electrochemical performance is using 3D nanostructured morphologies, since those materials display small charge transfer resistance and favorable ion transport within the 3D continuous framework (PANI e.g) (Shi et al. 2015). Expressive enhancements were observed for devices based on 3D nanostructured polypyrrole (Antonio et al. 2016, 2019).

Electrolytes

The electrolyte will play an important role in supercapacitors when pseudocapacitive materials are used, since the redox reactions occurring during charge/discharge require certain specificity from the electrolyte. Ions present in the electrolyte and the media pH are important for redox reactions, as already mentioned above for some examples. It is worth mentioning that most of the research on pseudocapacitive materials is performed using aqueous electrolyte, but the narrow electrochemical voltage window results in low energy density. In order to overcome this problem, pseudocapacitive materials can also be used with organic solvent-based electrolytes, mainly employing electrolytes also used in metal-ion batteries, since many of the pseudocapacitive material used in such configuration shows metal ion intercalation

(Augustyn et al. 2014, Choi et al. 2020). Conducting polymers have also been tested with ILs, showing different potentiodynamic profile than in aqueous electrolytes, due to the different activity in presence of such IL structure (Bazito et al. 2008). An asymmetrical capacitor using two different conducting polymer and aqueous gel electrolyte operating up to 1.6 V was also proposed, showing expanded operating voltage and capacitive behavior, in addition to the improved safety due to solid electrolyte (Kurra et al. 2015). Besides the enlarged operating voltage that non-aqueous electrolytes show, problems with lower capacitance must be overcome, especially when MXenes are employed. Such type of material shows outstanding capacitance in aqueous electrolyte but still fails when ILs are used. For instance, Ghidiu et al. (2014) reported a MXene of $Ti_3C_2T_x$ (T = OH, O or F) showing a gravimetric capacitance of 222 F g^{-1} in aqueous H_2SO_4 electrolyte (at 20 mV s^{-1}), or 821 F cm^{-3}. On the other hand, Lin et al. (2016) using a similar electrode preparation achivied only 70 F g^{-1} at the same 20 mV s^{-1} but using an ILs as electrolyte. That is more than three times higher capacitance when aqueous electrolyte is used.. In a different strategy, IL was dissolved in acetonitrile and used as electrolyte. As prepared MXene showed around 30 F g^{-1} at 20 mV s^{-1}, and the addition of carbon nanotubes to the electrode improved the gravimetric capacitance to around 75 F g^{-1} (Dall et al. 2016), which is still far lower than the aqueous counterpart.

MATERIALS DESIGN FOR ELECTROCHEMICAL ENERGY STORAGE

Electrode materials are the fundamental components in electrochemical energy storage devices, in both batteries and supercapacitors. In many cases, material selection plays an essential role in limiting the level of electric energy storage due to their theoretical specific capacity and their voltage. For either devices, the overall system performance relies on electroactivity and stability of electrode materials (Chen & Xue 2016). The main issues to address in the rational design of electrode materials are related to (i) energy density; (ii) kinetics of charge and mass transport; and (iii) structure stability *in operando* conditions.

For an electrode material with a given chemical composition, potential, structure stability, electronic conductivity, and charge transport are dependent on its crystal structure and the material's dimensionality. Different crystal structures present different atomic bonding and internal energy that can release different amounts of chemical energy. Moreover, when in nanometer scale, materials present a higher surface to volume ratio, which decreases the ion transport pathway and contributes to enhancing the capacity of electrodes. Nanostructured materials, such as hollow core/shell nanoparticles and nanowires, can also reduce electrode fatigue due to expansion/contraction during cyclability (Neto et al. 2020, Zhou et al. 2019a). In the following section, we will briefly present the most common procedures to synthesize electrode materials, and discuss the advantages and limitations related to each method. Table I summarizes some materials and the strategies used produce each of them.

Hydrothermal and solvothermal syntheses

Hydrothermal (in water) and solvothermal (in other solvents such as ethylene glycol or acetone) syntheses can be described as methods for formation and growth of crystals through a chemical reaction in a reactor sealed with a solution above ambient temperature and pressure (Feng & Xu 2001, Kharissova et al. 2019).

Table I. Materials for electrochemical energy storage devices prepared by different methods with different morphologies.

Material	Method	Morphology	Application	Ref.
C/ Fe_3O4	Microwave	Nanowires	Battery	(Muraliganth et al. 2009)
C/CoO	Reflux method	Nanoflakes	Battery	(Jiang et al. 2019)
C/$LiFePO_4$	Modified Pechini method	Porous nanoarchitecture	Battery	(Dimesso et al. 2011)
C/$W_{0.4}Mo_{0.6}O_3$ and C/WOx-MoO_2	Microwave	Nanorods	Battery	(Yoon & Manthiram 2011)
C/$ZnFe_2O_4$	Hydrothermal	Nanospheres	Battery	(Yao et al. 2017)
$Ca_9Co_{12}O_{28}$	Modified Pechini method	Nanoplates	Battery	(Zhou et al. 2019b)
Fe_2O_3	Hydrothermal	Nanorod	Battery	(Lin et al. 2011)
Graphite C/$LiCoO_2$	Mechanochemistry	Platelet-like	Battery	(Kwon, 2013)
$Li_{1.2}(Mn_{0.62}Ni_{0.38})_{0.8}O_2$	Co-precipitation	Core-shell	Battery	(Koenig et al. 2011)
$Li_{1.2}Mn_{0.54}Ni_{0.13}Co_{0.13}O_2$	Co-precipitation	Octahedral	Battery	(He et al. 2018)
$Li_{1+x}V_3O_8$ (x = 0.07/0.2)	Mechanochemistry	--	Battery	(Kosova & Devyatkina 2004)
$Li_4Ti_5O_{12}$	Hydrothermal	Flower-like	Battery	(Wang et al. 2015a)
$Li_4Ti_5O_{12}$-TiO_2	Oil/water interface method	Nanoflakes	Battery	(Liu et al. 2016)
$LiCoO_2$	Hydrothermal	Nanoflake	Battery	(Xia et al. 2019)
$LiCoPO_4$	Hydrothermal Pechini sol-gel	Orthorhombicprism Crystallized films	Battery	(Huang et al. 2005) (Bhuwaneswari et al. 2010)
$LiFePo_4$	Pechini method Mechanochemistry	--	Battery	(Yamada et al. 2001) (Kosova & Devyatkina 2004)
$LiMn_2O_4$	Calcination Mechanochemistry	-- Submicrometric cubes	Battery	(Thackeray et al. 1984) (Wei et al. 2014)
$LiMnPO_4$	Solvothermal	Nanorods Nanoplates Nanorods	Battery	(Qin et al. 2012)
$LiMnPO_4$/C	Pechini method	Nano-pyramid	Battery	(Ragupathi et al. 2019)
LiV_3O_8	Spray pyrolysis	Yolk–Shell	Battery	(Choi & Kang 2013)
$LiVPO_4F$	Carbothermal reduction	--	Battery	(Barker et al. 2005)
MnO_2	Precipitation	Needle-like	Supercapacitor	(Chen et al. 2009)

Table I. (continuation).

Material	Method	Morphology	Application	Ref.
$Nb_{16}W_5O_{55}$	Co-thermal oxidation	Superstructure	Battery	(Griffith et al. 2018)
$Nb_{18}W_{16}O_{93}$	Co-thermal oxidation	Superstructure	Battery	(Griffith et al. 2018)
Nb_2O_5	Hydrothermal	Nanowires Hollow microspheres	Supercapacitor	(Wang et al. 2015b) (Kong et al. 2016)
Nb_2O_5/C	Modified Pechini method	Mesoporous	Supercapacitor	(Lim et al. 2014)
Nb_2O_5@C	Hydrothermal	Core-shell	Supercapacitor	(Kong et al. 2016)
NbC/C	Electrospinning	Nanofibers	Supercapacitor and Battery	(Tolosa et al. 2016)
NbO_2@C	Hydrothermal	Core-shell	Supercapacitor	(Kong et al. 2016)
$NiCo_2O_4$	Microwave	Sheets	Battery and Supercapacitor	(Mondal et al. 2015)
N-TiO_2–B/NG	Hydrothermal	Sheets	Battery	(Han et al. 2017)
$Ti_2Nb_{10}O_{29-x}$	Solvothermal	Microspheres	Battery	(Deng et al. 2017) (Tang et al. 2014)
TiO_2	Hydrothermal	Nanotubular Nanowire	Battery	(Tang et al. 2014) (Armstrong et al. 2005)
TiO_2-graphene	Hydrothermal	Sheets	Battery	(Yang et al. 2009)
ZIF8	Aqueous Reflux Mechanochemistry	Nanocrystals Crystals	Battery	(Pan et al. 2011) (Beldon et al. 2010)
$ZnFe_2O_4$	Co-precipitation	Nanorods	Battery	(Zhong et al. 2016)

Among all methods, hydrothermal and solvothermal syntheses are ideal for controlling the morphology, particle size distribution, shape, uniformity, area, crystallinity, nucleation, and a technique to facilitate an excellent reproducibility of nanomaterials especially one to three-dimensional nanocrystals (Kharissova et al. 2019, Shi et al. 2013). The precise control over hydrothermal and solvothermal conditions is indispensable for the preparation of structures. These parameters can be controlled and involve changing pressure, pH, temperature, solvent, organic additives, reaction time, and the precursor source (Byrappa & Adschiri 2007, Kharissova et al. 2019, Shi et al. 2013). Under this scenario, the hydrothermal and solvothermal syntheses would greatly influence the performance of electrochemical energy storage/conversion applications.

Co-precipitation method

Together with hydrothermal, the co-precipitation method is one of the most traditional processes to prepare transition metal oxides, and it involves

the formation of insoluble products of inorganic oxides. Two strategies are mainly used, where one is the proper metal oxide directly precipitated and the other occurs with an intermediated by-product precipitation followed by oxide crystallization upon temperature treatment. This method is versatile to produce 1,2,3-d transition metal oxide structures and allows the combination with other methodologies to reach desired crystalline phases, sizes, and morphologies.

Koenig et al. (2011) have tailored lithiated manganese and nickel oxides in a reactor system with NH_4OH/Na_2CO_3 for LIB cathode. Their report on the internal gradient of composition presented excellent retention of discharge capacity over 100 cycles. He et al. (2018) reported octahedral $Li_{1.2}Mn_{0.54}Ni_{0.13}Co_{0.13}O_2$ core-shell Li-rich with a spinel-layer via co-precipitation/gel method. According to the authors, the LIB cathodic material contained enough oxygen vacancies in the lattice allowing the reinsertion of Li^+ (He et al. 2018). Compared to the traditional co-precipitation material, the proposed co-precipitation/gel approach yielded higher discharge capacity and coulombic efficiency.

Sol-gel method

The sol-gel method is an alternative to hydrothermal and solvothermal synthesis, it offers some particular advantages to produce complex inorganic materials at lower temperature and pressure, and shorter synthesis times (Danks et al. 2016). Moreover, sol-gel chemistry is capable of controlling the morphology and the size of particles (Haetge et al. 2012, Trewyn et al. 2007). The sol-gel method implies hydrolysis and condensation of a metal alkoxide precursor to obtain a sol composed of colloidal particles and, finally, an interconnect rigid network structure called a gel (Danks et al. 2016, Hench & West 1990, Lakshmi et al. 1997). In the sol-gel chemistry, there are many different ways to control the structures with small changes in conditions relatively easy to achieve as pH, the metal alkoxide/H_2O ratio, and temperature (Hench & West 1990).

Pechini method

The Pechini method (Pechini 1967) (and its modified approaches) is versatile, capable of fine engineering the material surface, and it overcomes most of the difficulties and disadvantages of traditional alkoxide based sol-gel process (Dimesso 2016). The synthesis follows two major steps to achieve oxide structures: *i)* A desired cation polyesterification resin is generated by the combination of the chosen metal precursor and hydroxycarboxylic acid to polyhydroxy alcohol. The cationic-species homogeneity is guaranteed by choosing a soluble/time-stable precursors and heating the solution at mild temperatures. *ii)* Calcination of the resin. The evaporation of the organics is conducted upon a thermal treating step, resulting in the crystallization of the desired oxide. Different Pechini-modified approaches are found to achieve desirable structural characteristics in the nanomaterials (Dimesso et al. 2011).

Chemical vapor deposition method

The chemical vapor deposition method can be considered as a gas-phase synthetic process. In vapor phase, the mechanism of formation can be divided into three main events: precursor vaporization, nucleation, and growth of crystals. This approach is very simple, versatile, and also operates continuously with high product yield for desired nanoparticle preparation (Maduraiveeran et al. 2019). However, to produce materials with controlled morphology, it is required to use a template or to modify the substrate to allow nanostructures to grow (Zhou

et al. 2019a). The multistep deposition of metals or metal oxides offers an alternative to produce multilayered electrochemical devices.

Microwave irradiation method

Microwave irradiation is another interesting tool to produce metal oxides for not depending on high pressure or temperature. Particularly, this method stands out by its simplicity and rapidity with which reactions occur, besides being a methodology that allows scale-up without heat diffusion problems (Herring et al. 2013). The microwave heating depends on the reactants ability to adsorb such irradiation. Generally, irradiated metal precursors with a large microwave irradiation absorption feature tend to reach the effective temperature instantaneously, allowing them to achieve small nanoparticles in a fast way.

Mechanochemical synthesis

Mechanochemistry has emerged as one of the alternatives to conventional solvent and thermal-based routes for chemistry and materials preparation (James et al. 2012). It has been highlighted as one of the innovative world changing technologies by IUPAC (Gomollón-Bel 2019). Apart from the ancient use in minerals and metallurgic sciences (Baláž et al. 2013, Suryanarayana 2001), by using mechanical energy one can induce organic reactions (Wang 2013), co-crystal formation (Braga et al. 2013, Fischer et al. 2015), coordinate frameworks (Gualteros et al. 2019, Mottillo & Friščić 2017) and phase transitions (Descamps & Willart 2016, Oliveira et al. 2018). Ball milling devices are the most common apparatuses used for such a purpose, enabling to generate materials for several applications with eco-friendly based protocols, as most of the reactions are carried out directly in the solid state. In this procedure, the raw reactant materials, mostly powders, are introduced in the milling jars along with balls as milling bodies. As the milling starts, mixing and comminution occurs, i.e. the breakdown of the solids into smaller objects, increasing the surface area of the overall system. Concomitantly, the accumulation of stress in the solid particles in the form of plastic deformation and defects and the continuous generation of fresh reactive surfaces lead to the chemical transformations in reactive mixtures. The ongoing milling enhances these described processes and may push, many times, the reactions to completion in shorter times when compared to classical thermal routes. The ball to powder mass ratio and the type of mill (planetary ball mill, vibratory ball mill, attritor) (Baláž et al. 2013) influence the effectiveness of the milling in terms towards the desired product. The type of mechanical energy input (shock, impact, shear stress) can also drive to different products (Michalchuk et al. 2013).

In the electrochemistry field, mechanochemistry has been used for the elaboration of electrocatalysts such as nanoparticles, and materials for batteries and supercapacitors (Kosova & Devyatkina 2004, 2012, Kosova 2010, Muñoz-Batista et al. 2018, Ning et al. 2004, Tarascon et al. 2005). Fine particulate compounds used as electrodes with spinel, layered, framework structure and other amorphous materials were synthesized and tested as negative and positive electrodes and solid electrolytes (Kosova, 2010, Lenain et al. 1998, Soiron et al. 2001, Tarascon et al. 2005, Yang et al. 2010).

MXenes

The production of 2D materials can be classified into two different approaches, the bottom-up, which relies on the reaction of molecular building blocks to form covalently linked sheets, and the top-down, that consists of the chemical or mechanical exfoliation of bulk crystal to

obtain individual sheets (Zhang et al. 2016). The latter approach is the most used for the production of graphene and graphene-analog materials, such as molybdenum disulfide (Mo_2S) and hexagonal boron nitride, because the interlayer interactions are much weaker than the bonds within the layers (Nicolosi et al. 2013).

In the case of MXenes, etching of MAX phases followed by exfoliation is the most common strategy of synthesis, and several etching methods have been reported in the literature (Alhabeb et al. 2017a, Naguib et al. 2012, Verger et al. 2019a, 2019b). The first reported MXene was $Ti_3C_2T_x$ and was produced by etching Al atoms in Ti_3AlC_2 with concentrated hydrofluoric acid (HF) for few hours at room temperature (Naguib et al. 2011). To date, over 30 MXenes have been synthesized, and new ones are yet to be discovered, since only about 20% of known MAX phases available have been successfully etched (Verger et al. 2019a).

Etching conditions depend on HF concentration, frequently from 5 to 30 wt%, or on the formation of HF *in situ* by using LiF in acidic media (Ghidiu et al. 2014, Peng et al. 2016) or using NH_4HF_2 (Halim et al. 2014, Lipatov et al. 2016). To obtain individual sheets of $Ti_3C_2T_x$, depending on the etching protocol, it is required to use intercalating compounds to expand interlayer space in MXene flakes. When lithium fluoride is employed as an etchant, solvated Li^+ ion intercalation can be adjusted, and delamination of individual sheets can be achieved by sonication in 5 mol L^{-1} LiF/ 6 mol L^{-1} HCl, or by manual shaking in 12 mol L^{-1} LiF/ 9 mol L^{-1} HCl (Sang et al. 2016), called minimally intensive layer delamination (MILD). The MILD method is more suitable for applications where larger and less defective MXene sheets are required (Sang et al. 2016). When harsh etching conditions are employed, such as 30 wt % of HF, MAX phases expand during the process and accordion-like structures were formed (Figure 5c), while 5 wt % HF, NH_4F, and MILD-etched delamination produced negligible opening in MXenes lamellas (Alhabeb et al. 2017b).

Despite the extraordinary properties of MXene materials, there are some concerns regarding the potential hazards during their synthesis and processing (Lakhe et al. 2019) (Figure 5), which remains as one of the main drawbacks that hinder scaling up their production. Hazards related to MXene synthesis includes handling toxic and corrosive reactants, and also the production of potentially explosive by products, such as H_2 (Lakhe et al. 2019). Properly wash MXene is another important problem to address, because fluoride is not completely removed after the synthesis, the exposure to nanostructured materials with high surface area with hazardous functional groups is of great concern to human health (Fadeel et al. 2018). The large-scale production of MXenes and its application in functional devices will only be achieve when safety considerations were better understood, from raw materials until its final disposal.

CONCLUSIONS

In the present part of this review series, it was intended to show the importance that electrochemical energy storage technologies have gained after decades of development that culminated on the Nobel Prize 2019 in Chemistry. Particularly, electrochemical capacitors were explored, highlighting their fundamental difference when compared to batteries. Different types of electrochemical capacitors were explored: double-layer capacitor and pseudocapacitive capacitors, including metal oxides, MXenes and conducting polymers. In addition, this part also explored

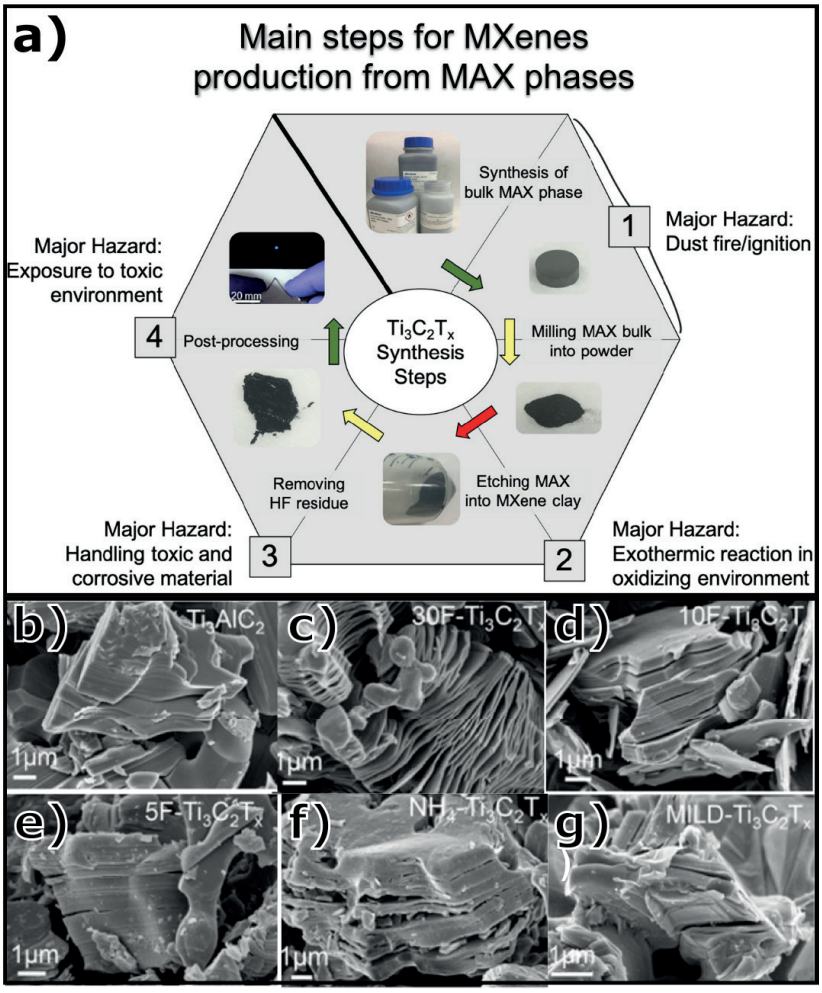

Figure 5. Schematic representation of MXene production from raw materials (a). The major risk associated to each step is highlighted in the box. Reprinted (adapted) with permission from ref (Lakhe et al. 2019). Copyright 2019, The American Chemical Society. Representative SEM images of (b) Ti_3AlC_2 (MAX) and (c-g) $Ti_3C_2T_x$ (MXenes) obtained in different etching conditions. Multilayered structures were synthesized with: c) 30 wt %, d) 20 wt %, and e) 5 wt % of HF; f) ammonium hydrogen fluoride (NH_4HF_2), and g) 10 mol L^{-1} LiF in 9 mol L^{-1} HCl. Reprinted (adapted) with permission from ref (Alhabeb et al. 2017a). Copyright 2017, The American Chemical Society.

the most common strategies and synthetic routes to obtain nanostructured materials to be applied in both electrochemical capacitors and batteries. The next part of the review will address the advances in rechargeable batteries.

List of acronyms

PANI: polyaniline.
EDLC: electrochemical double-layer capacitor.
AC: activated carbon.
TEA^+: tetraethylammonium cation.
TMA^+: tetramethylammonium cation.
IL: ionic liquid.
$Im_{x,y,z}^+$: imidazolium-based cation, where *x,y,z* denotes for the length of alkyl chains.
$Pyr_{x,y,}^+$: pyrrolidinium-based cation, where *x,y* denotes for the length of alkyl chains.
$Pip_{x,y,}^+$: piperidinium-based cation, where *x,y* denotes for the length of alkyl chains.
$N_{x,y,z,w}^+$: ammonium-based cation, where *x,y,z,w* denotes for the length of alkyl chains.
$P_{x,y,z,w}^+$: phosponium-based cation, where *x,y,z,w* denotes for the length of alkyl chains.
$S_{x,y,z}^+$: sulfonium-based cation, where *x,y,z* denotes for the length of alkyl chains.
Tf_2N^-: bis(trifluoromethylsulfonyl) imide anion.
FSI^-: bis(fluorosulfonyl)imide anion.
$Im_{1,2}^+$: 1-ethyl-3-methyl imidazolium cation.
$Pyr_{1,4}^+$: *N*-methyl-*N*-methyl pyrrolidinium.
$Azp_{x,y}^+$: azepanium-based cation, where *x,y* denotes for the length of alkyl chains.

TMO: transition metal oxide.
MXenes: 2D transition metal carbides, nitrides or carbonitrides.
MAX: M is for a transition metal, A for an element from group A and X is carbon or nitrogen.
PPy: polypyrrolye.
PTh: polythiofene.
PEDOT: poly(3,4-ethylenedioxythiophene).
MILD: minimally intensive layer delamination.

Acknowledgments

This work was supported by the Conselho Nacional de Desenvolvimento Científico e Tecnológico (CNPq, 303141/2017-4), Coordenação de Aperfeiçoamento de Pessoal de Nível Superior (CAPES) and Fundação de Amparo à Pesquisa do Estado de São Paulo (FAPESP, 2015/26308-7). VLM (13/22748-7), IEM (17/20043-7), MML (19/02669-1), PFMO (17/15456-0), RMA (17/15469-5), SC (18/11320-0), WGM (18/23072-0), TTO (17/10046-9) and BLS (19/09341-1) wish to thank FAPESP for scholarships. ECM (88882.328255/2019-01) thanks CAPES for scholarship.

REFERENCES

ABBAS Q, RAZA R, SHABBIR I & OLABI AG. 2019. Heteroatom doped high porosity carbon nanomaterials as electrodes for energy storage in electrochemical capacitors: A review. J Sci Adv Mater Devices 4: 341-352.

AHN YR, SONG MY, JO SM, PARK CR & KIM DY. 2006. Electrochemical capacitors based on electrodeposited ruthenium oxide on nanofibre substrates. Nanotechnology 17: 2865-2869.

ALHABEB M, MALESKI K, ANASORI B, LELYUKH P, CLARK L, SIN S & GOGOTSI Y. 2017a. Guidelines for Synthesis and Processing of Two-Dimensional Titanium Carbide (Ti3C2Tx MXene). Chem Mater 29: 7633-7644.

ALHABEB M, MALESKI K, ANASORI B, LELYUKH P, CLARK L, SIN S & GOGOTSI Y. 2017b. Guidelines for Synthesis and Processing of Two-Dimensional Titanium Carbide (Ti3C2Tx MXene). Chem Mater 29: 7633-7644.

ANTONIO JLS, HÖFLER L, LINDFORS T & CÓRDOBA DE TORRESI SI. 2016. Electrocontrolled Swelling and Water Uptake of a Three-Dimensional Conducting Polypyrrole Hydrogel. ChemElectroChem 3: 2146-2152.

ANTONIO JLS, MARTINS VL, CÓRDOBA DE TORRESI SI & TORRESI RM. 2019. QCM-D study of electrochemical synthesis of 3D polypyrrole thin films for negative electrodes in supercapacitors. Electrochim Acta 324: 134887.

ARDIZZONE S, FREGONARA G & TRASATTI S. 1990. "Inner" and "outer" active surface of RuO2 electrodes. Electrochim Acta 35: 263-267.

ARMSTRONG AR, ARMSTRONG G, CANALES J, GARCÍA R & BRUCE PG. 2005. Lithium-ion intercalation into TiO2-B nanowires. Adv Mater 17: 862-865.

AUGUSTYN V, SIMON P & DUNN B. 2014. Pseudocapacitive oxide materials for high-rate electrochemical energy storage. Energy Environ Sci 7: 1597-1614.

AYALNEH TIRUYE G, MUÑOZ-TORRERO D, PALMA J, ANDERSON M & MARCILLA R. 2015. All-solid state supercapacitors operating at 3.5 V by using ionic liquid based polymer electrolytes. J Power Sources 279: 472-480.

BALÁŽ P ET AL. 2013. Hallmarks of mechanochemistry: from nanoparticles to technology. Chem Soc Rev 42: 7571-7637.

BANERJEE J, DUTTA K, KADER MA & NAYAK SK. 2019. An overview on the recent developments in polyaniline-based supercapacitors. Polym Adv Technol 30: 1902-1921.

BARKER J, GOVER RKB, BURNS P, BRYAN A, SAIDI MY & SWOYER JL. 2005. Structural and electrochemical properties of lithium vanadium fluorophosphate, LiVPO4F. J Power Sources 146: 516-520.

BAZITO FFC, SILVEIRA LT, TORRESI RM & CÓRDOBA DE TORRESI SI. 2008. On the stabilization of conducting pernigraniline salt by the synthesis and oxidation of polyaniline in hydrophobic ionic liquids. Phys Chem Chem Phys 10: 1457-1462.

BEGUIN F & FRACKOWIAK E. 2013. Supercapacitors Materials, Systems, and Applications. 1st ed., Weinheim: Wiley-VCH Verlag GmbH & Co.

BÉGUIN F, PRESSER V, BALDUCCI A & FRACKOWIAK E. 2014. Carbons and Electrolytes for Advanced Supercapacitors. Adv Mater 26: 2219-2251.

BELDON PJ, FÁBIÁN L, STEIN RS, THIRUMURUGAN A, CHEETHAM AK & FRIŠČIĆ T. 2010. Rapid Room-Temperature Synthesis of Zeolitic Imidazolate Frameworks by Using Mechanochemistry. Angew Chemie Int Ed 49: 9640-9643.

BHUWANESWARI MS, DIMESSO L & JAEGERMANN W. 2010. Preparation of LiCoPO4 powders and films via sol-gel. J Sol-Gel Sci Technol 56: 320-326.

BRAGA D, MAINI L & GREPIONI F. 2013. Mechanochemical preparation of co-crystals. Chem Soc Rev 42: 7638-7648.

BROUSSE T, CROSNIER O & BÉLANGER D. 2017. Capacitive and Pseudocapacitive Electrodes for Electrochemical

Capacitors and Hybrid Devices. In: Met. Oxides Supercapacitors. 1st ed., Amsterdam: Elsevier. 1-21.

BYRAPPA K & ADSCHIRI T. 2007. Hydrothermal technology for nanotechnology. Prog Cryst Growth Charact Mater 53: 117-166.

CAI M, OUTLAW RA, QUINLAN RA, PREMATHILAKE D, BUTLER SM & MILLER JR. 2014. Fast response, vertically oriented graphene nanosheet electric double layer capacitors synthesized from C2H2. ACS Nano 8: 5873-5882.

CANDELARIA SL, GARCIA BB, LIU D & CAO G. 2012. Nitrogen modification of highly porous carbon for improved supercapacitor performance. J Mater Chem 22: 9884-9889.

CHEN CH, WASHBURN N & GEWIRTH AA. 1993. In situ atomic force microscope study of Pb underpotential deposition on Au(111): Structural properties of the catalytically active phase. J Phys Chem 97: 9754-9760.

CHEN D, WANG Q, WANG R & SHEN G. 2015. Ternary oxide nanostructured materials for supercapacitors: a review. J Mater Chem A 3: 10158-10173.

CHEN K & XUE D. 2016. Materials chemistry toward electrochemical energy storage. J Mater Chem A 4: 7522-7537.

CHEN S, ZHU J, HAN Q, ZHENG Z, YANG Y & WANG X. 2009. Shape-controlled synthesis of one-dimensional MnO2 via a facile quick-precipitation procedure and its electrochemical properties. Cryst Growth Des 9: 4356-4361.

CHMIOLA J, LARGEOT C, TABERNA PL, SIMON P & GOGOTSI Y. 2008. Desolvation of ions in subnanometer pores and its effect on capacitance and double-layer theory. Angew Chemie - Int Ed 47: 3392-3395.

CHOI C, ASHBY DS, BUTTS DM, DEBLOCK RH, WEI Q, LAU J & DUNN B. 2020. Achieving high energy density and high power density with pseudocapacitive materials. Nat Rev Mater 5: 5-19.

CHOI SH & KANG YC. 2013. Excellent electrochemical properties of Yolk-Shell LiV3O 8 powder and its potential as cathodic material for lithium-ion batteries. Chem - A Eur J 19: 17305-17309.

CONWAY BE. 1991. Transition from "Supercapacitor" to "Battery" Behavior in Electrochemical Energy Storage. J Electrochem Soc 138: 1539-1548.

CONWAY BE. 1999. Electrochemical Supercapacitors: Scientific Fundamentals and Technological Applications. New York: Kluwer Academic/Plenum Publishing.

CONWAY BE, BIRSS V & WOJTOWICZ J. 1997. The role and utilization of pseudocapacitance for energy storage by supercapacitors. J Power Sources 66: 1-14.

DALL Y, ROZIER P, TABERNA P, GOGOTSI Y & SIMON P. 2016. Capacitance of two-dimensional titanium carbide (MXene) and MXene / carbon nanotube composites in organic electrolytes. J Power Sources 306: 510-515.

DANKS AE, HALL SR & SCHNEPP Z. 2016. The evolution of 'sol-gel' chemistry as a technique for materials synthesis. Mater Horizons 3: 91-112.

DE ALBUQUERQUE MARANHÃO SL & TORRESI RM. 1999a. Anion and Solvent Exchange as a Function of the Redox States in Polyaniline Films. J Electrochem Soc 146: 4179.

DE ALBUQUERQUE MARANHÃO SL & TORRESI RM. 1999b. Quartz crystal microbalance study of charge compensation process in polyaniline films doped with surfactant anions. Electrochim Acta 44: 1879-1885.

DENG S ET AL. 2017. Ti2Nb10O29-x mesoporous microspheres as promising anode materials for high-performance lithium-ion batteries. J Power Sources 362: 250-257.

DESCAMPS M & WILLART JF. 2016. Perspectives on the amorphisation/milling relationship in pharmaceutical materials. Adv Drug Deliv Rev 100: 51-66.

DIMESSO L, SPANHEIMER C, JACKE S & JAEGERMANN W. 2011. Synthesis and characterization of LiFePO4/3-dimensional carbon nanostructure composites as possible cathode materials for Li-ion batteries. Ionics 17: 429-435.

DIMESSO L. 2016. Pechini Processes: An Alternate Approach of the Sol-Gel Method, Preparation, Properties, and Applications. In: Handb Sol-Gel Sci Technol Cham: Springer International Publishing. 1-22.

DUBAL DP, DHAWALE DS, SALUNKHE RR, PAWAR SM & LOKHANDE CD. 2010. A novel chemical synthesis and characterization of Mn 3 O 4 thin films for supercapacitor application. Appl Surf Sci 256: 4411-4416.

EFTEKHARI A. 2017. Supercapacitors utilising ionic liquids. Energy Storage Mater 9: 47-69.

FADEEL B. et al. 2018. Advanced tools for the safety assessment of nanomaterials. Nat Nanotechnol 13: 537-543.

FAN LZ & MAIER J. 2006. High-performance polypyrrole electrode materials for redox supercapacitors. Electrochem Commun 8: 937-940.

FENG S & XU R. 2001. New Materials in Hydrothermal Synthesis. Acc Chem Res 34: 239-247.

FIC K, PŁATEK A, PIWEK J, MENZEL J, ŚLESIŃSKI A, BUJEWSKA P, GALEK P & FRĄCKOWIAK E. 2019. Revisited insights into charge storage mechanisms in electrochemical capacitors with Li2SO4-based electrolyte. Energy Storage Mater 22: 1-14.

FISCHER F, SCHOLZ G, BATZDORF L, WILKE M & EMMERLING F. 2015. Synthesis, structure determination, and formation of a theobromine : oxalic acid 2 : 1 cocrystal. CrystEngComm 17: 824-829.

GAGLIARDI LG, CASTELLS CB, RÀFOLS C, ROSÉS M & BOSCH E. 2007. Static Dielectric Constants of Acetonitrile/Water Mixtures at Different Temperatures and Debye–Hückel A and a 0 B Parameters for Activity Coefficients. J Chem Eng Data 52: 1103-1107.

GHIDIU M, LUKATSKAYA MR, ZHAO MQ, GOGOTSI Y & BARSOUM MW. 2014. Conductive two-dimensional titanium carbide 'clay' with high volumetric capacitance. Nature 516: 78-81.

GOMOLLÓN-BEL F. 2019. Ten Chemical Innovations That Will Change Our World: IUPAC identifies emerging technologies in Chemistry with potential to make our planet more sustainable. Chem Int 41: 12-17.

GONZÁLEZ A, GOIKOLEA E, BARRENA JA & MYSYK R. 2016. Review on supercapacitors: Technologies and materials. Renew Sustain Energy Rev 58: 1189-1206.

GRIFFITH KJ, WIADEREK KM, CIBIN G, MARBELLA LE & GREY CP. 2018. Niobium tungsten oxides for high-rate lithium-ion energy storage. Nature 559: 556-563.

GUALTEROS JAD ET AL. 2019. Synthesis of highly dispersed gold nanoparticles on Al2O3, SiO2, and TiO2 for the solvent-free oxidation of benzyl alcohol under low metal loadings. J Mater Sci 54: 238-251.

HAETGE J, DJERDJ I & BREZESINSKI T. 2012. Nanocrystalline NiMoO4 with an ordered mesoporous morphology as potential material for rechargeable thin film lithium batteries. Chem Commun 48: 6726-6728.

HALIM J ET AL. 2014. Transparent Conductive Two-Dimensional Titanium Carbide Epitaxial Thin Films. Chem Mater 26: 2374-2381.

HALL PJ, MIRZAEIAN M, FLETCHER SI, SILLARS FB, RENNIE AJR, SHITTA-BEY GO, WILSON G, CRUDEN A & CARTER R. 2010. Energy storage in electrochemical capacitors: designing functional materials to improve performance. Energy Environ Sci 3: 1238-1251.

HAN Z, PENG J, LIU L, WANG G, YU F & GUO X. 2017. Few-layer TiO2-B nanosheets with N-doped graphene nanosheets as a highly robust anode for lithium-ion batteries. RSC Adv 7: 7864-7869.

HENCH LL & WEST JK. 1990. The sol-gel process. Chem Rev 90: 33-72.

HER LJ, HONG JL & CHANG CC. 2006. Preparation and electrochemical characterizations of poly(3,4-dioxyethylenethiophene)/LiCoO2-Ketjenblack composite cathode in lithium-ion battery. J Power Sources 161: 1247-1253.

HERRING NP, PANDA AB, ABOUZEID K, ALMAHOUDI SH, OLSON CR, PATEL A & EL-SHALL MS. 2013. Microwave Synthesis of Metal Oxide Nanoparticles. In: Met Oxide Nanomater Chem Sensors. New York. Springer, p. 245-284.

HE W ET AL. 2018. Coprecipitation-Gel Synthesis and Degradation Mechanism of Octahedral Li1.2Mn0.54Ni0.13Co0.13O2 as High-Performance Cathode Materials for Lithium-Ion Batteries. ACS Appl Mater Interfaces 10: 23018-23028.

HUANG X, MA J, WU P, HU Y, DAI J, ZHU Z, CHEN H & WANG H. 2005. Hydrothermal synthesis of LiCoPO4 cathode materials for rechargeable lithium ion batteries. Mater Lett 59: 578-582.

HUGUENIN F & TORRESI RM. 2008. Investigation of the Electrical and Electrochemical Properties of Nanocomposites from V2O5, Polypyrrole, and Polyaniline. J Phys Chem C 112: 2202-2209.

JÄCKEL N, SIMON P, GOGOTSI Y & PRESSER V. 2016. Increase in Capacitance by Subnanometer Pores in Carbon. ACS Energy Lett 1: 1262-1265.

JAMES SL ET AL. 2012. Mechanochemistry: opportunities for new and cleaner synthesis. Chem Soc Rev 41: 413-447.

JIANG J, MA C, MA T, ZHU J, LIU J, YANG G & YANG Y. 2019. A novel CoO hierarchical morphologies on carbon nanofiber for improved reversibility as binder-free anodes in lithium/sodium ion batteries. J Alloys Compd 794: 385-395.

JIANG J & KUCERNAK A. 2002. Electrochemical supercapacitor material based on manganese oxide: Preparation and characterization. Electrochim Acta 47: 2381-2386.

JIANG Y & LIU J. 2019. Definitions of Pseudocapacitive Materials: A Brief Review. Energy Environ Mater 2: 30-37.

KANDALKAR SG ET AL. 2010. Preparation and electrochemical properties of lamellar MnO2 for supercapacitors. Appl Surf Sci 255: 5540-5544.

KANDALKAR SG, GUNJAKAR JL & LOKHANDE CD. 2008. Preparation of cobalt oxide thin films and its use in supercapacitor application. Appl Surf Sci 254: 5540-5544.

KARAMI H, MOUSAVI MF & SHAMSIPUR M. 2003. A new design for dry polyaniline rechargeable batteries. J Power Sources 117: 255-259.

KHARISSOVA OV, KHARISOV BI, OLIVA GONZÁLEZ CM, MÉNDEZ YP & LÓPEZ I. 2019. Greener synthesis of chemical compounds and materials. R Soc Open Sci 6: 191378.

KHOLMANOV IN ET AL. 2013. Reduced graphene oxide/copper nanowire hybrid films as high performance transparent electrodes. ACS Nano 7: 1811-1816.

KIM D, SHIN G, KANG YJ, KIM W & HA JS. 2013. Fabrication of a Stretchable Solid-State Micro-Supercapacitor Array. ACS Nano 7: 7975-7982.

KIM JW, AUGUSTYN V & DUNN B. 2012. The Effect of Crystallinity on the Rapid Pseudocapacitive Response of Nb2O5. Adv Energy Mater 2: 141-148.

KOENIG GM, BELHAROUAK I, DENG H, SUN YK & AMINE K. 2011. Composition-Tailored Synthesis of Gradient Transition Metal Precursor Particles for Lithium-Ion Battery Cathode Materials. Chem Mater 23: 1954-1963.

KONG L, ZHANG C, WANG J, QIAO W, LING L & LONG D. 2016. Nanoarchitectured Nb2O5 hollow, Nb2O5 @carbon and NbO2 @carbon Core-Shell Microspheres for Ultrahigh-Rate Intercalation Pseudocapacitors. Sci Rep 6: 1-10.

KOSOVA NV. 2010. Soft mechanochemical synthesis of materials for lithium-ion batteries: principles and applications. In: High-Energy Ball Milling. Woodhead Publishing. 331-360.

KOSOVA N & DEVYATKINA E. 2004. On mechanochemical preparation of materials with enhanced characteristics for lithium batteries. Solid State Ionics 172: 181-184.

KOSOVA NV & DEVYATKINA ET. 2012. Synthesis of nanosized materials for lithium-ion batteries by mechanical activation. Studies of their structure and properties. Russ J Electrochem 48: 320-329.

KUMAR KS, CHOUDHARY N, JUNG Y & THOMAS J. 2018. Recent Advances in Two-Dimensional Nanomaterials for Supercapacitor Electrode Applications. ACS Energy Lett 3: 482-495.

KUO SL & WU NL. 2006. Electrochemical characterization on MnFe2O4/carbon black composite aqueous supercapacitors. J Power Sources 162: 1437-1443.

KURRA N, WANG R & ALSHAREEF HN. 2015. All conducting polymer electrodes for asymmetric solid-state supercapacitors. J Mater Chem A 3: 7368-7374.

KWON NH. 2013. The effect of carbon morphology on the LiCoO2 cathode of lithium ion batteries. Solid State Sci 21: 59-65.

LAFORGUE A, SIMON P, FAUVARQUE JF, SARRAU JF & LAILLER P. 2002. Hybrid Supercapacitors Based on Activated Carbons and Conducting Polymers. J Electrochem Soc 148: A1130.

LAKHE P, PREHN EM, HABIB T, LUTKENHAUS JL, RADOVIC M, MANNAN MS & GREEN MJ. 2019. Process Safety Analysis for Ti3C2Tx MXene Synthesis and Processing Ind Eng Chem Res 58: 1570-1579.

LAKSHMI BB, DORHOUT PK & MARTIN CR. 1997. Sol-Gel Template Synthesis of Semiconductor Nanostructures. Chem Mater 9: 857-862.

LÉ T, BIDAN G, GENTILE P, BILLON F, DEBIEMME-CHOUVY C, PERROT H, SEL O & ARADILLA D. 2019. Understanding the energy storage mechanisms of poly(3,4-ethylenedioxythiophene)-coated silicon nanowires by electrochemical quartz crystal microbalance. Mater Lett 240: 59-61.

LEE HY &, GOODENOUGH JB. 1999. Supercapacitor Behavior with KCl Electrolyte. J Solid State Chem 144: 220-223.

LEE JW, HALL AS, KIM JD & MALLOUK TE. 2012. A facile and template-free hydrothermal synthesis of Mn 3O 4 nanorods on graphene sheets for supercapacitor electrodes with long cycle stability. Chem Mater 24: 1158-1164.

LENAIN C, AYMARD L & TARASCON JM. 1998. Electrochemical properties of Mg2Ni and Mg2Ni2 prepared by mechanical alloying. J Solid State Electrochem 2: 285-290.

LIM E ET AL. 2014. Advanced hybrid supercapacitor based on a mesoporous niobium pentoxide/carbon as high-performance anode. ACS Nano 8: 8968-8978.

LIN YM, ABEL PR, HELLER A & MULLINS CB. 2011. α-Fe2O3 nanorods as anode material for lithium ion batteries. J Phys Chem Lett 2: 2885-2891.

LIN Z, BARBARA D, TABERNA PL, VAN AKEN KL, ANASORI B, GOGOTSI Y & SIMON P. 2016. Capacitance of Ti3C2Tx MXene in ionic liquid electrolyte. J Power Sources 326: 575-579.

LIN Z, GOIKOLEA E, BALDUCCI A, NAOI K, TABERNA PL, SALANNE M, YUSHIN G & SIMON P. 2018a. Materials for supercapacitors: When Li-ion battery power is not enough. Mater Today 21: 419-436.

LIN Z, TABERNA PL & SIMON P. 2018b. Advanced analytical techniques to characterize materials for electrochemical capacitors. Curr Opin Electrochem 9: 18-25.

LIPATOV A, ALHABEB M, LUKATSKAYA MR, BOSON A, GOGOTSI Y & SINITSKII A. 2016. Effect of Synthesis on Quality, Electronic Properties and Environmental Stability of Individual Monolayer Ti3C2 MXene Flakes. Adv Electron Mater 2: 1600255.

LIU G, LIU X, WANG L, MA J, XIE H, JI X, GUO J & ZHANG R. 2016. Hierarchical Li4Ti5O12-TiO2 microspheres assembled from nanoflakes with exposed Li4Ti5O12 (011) and anatase TiO2 (001) facets for high-performance lithium-ion batteries. Electrochim Acta 222: 1103-1111.

LOPES LC, DA SILVA LC, VAZ BG, OLIVEIRA ARM, OLIVEIRA MM, ROCCO MLM, ORTH ES & ZARBIN AJG. 2018. Facile room temperature synthesis of large graphene sheets from simple molecules. Chem Sci 9: 7297-7303.

LUKATSKAYA MR ET AL. 2013. Cation intercalation and high volumetric capacitance of two-dimensional titanium carbide. Science 341: 1502-1505.

MACFARLANE DR, FORSYTH SA, GOLDING J & DEACON GB. 2002. Ionic liquids based on imidazolium, ammonium and pyrrolidinium salts of the dicyanamide anion. Green Chem 4: 444-448.

MACFARLANE DR ET AL. 2016. Ionic liquids and their solid-state analogues as materials for energy generation and storage. Nat Rev Mater 1: 15005.

MADURAIVEERAN G, SASIDHARAN M & JIN W. 2019. Earth-abundant transition metal and metal oxide nanomaterials: Synthesis and electrochemical applications. Prog Mater Sci 106: 100574.

MAIA G, TORRESI RM, TICIANELLI EA & NART FC. 1996. Charge Compensation Dynamics in the Redox Processes of Polypyrrole-Modified Electrodes. J Phys Chem 100: 15910-15916.

MARTINS VL, RENNIE AJR, LESOWIEC J, TORRESI RM & HALL PJ. 2017b. Using Polymeric Ionic Liquids as an Active Binder in Supercapacitors. J Electrochem Soc 164: A3253-A3258.

MARTINS VL, RENNIE AJR, SANCHEZ-RAMIREZ N, TORRESI RM & HALL PJ. 2018a. Improved Performance of Ionic Liquid Supercapacitors by using Tetracyanoborate Anions. ChemElectroChem 5: 598-604.

MARTINS VL, RENNIE AJR, TORRESI RM & HALL PJ. 2017a. Ionic liquids containing tricyanomethanide anions: physicochemical characterisation and performance as electrochemical double-layer capacitor electrolytes. Phys Chem Chem Phys 19: 16867-16874.

MARTINS VL & TORRESI RM. 2018. Ionic liquids in electrochemical energy storage. Curr Opin Electrochem 9: 26-32.

MARTINS VL, TORRESI RM & RENNIE AJR. 2018b. Design considerations for ionic liquid based electrochemical double layer capacitors. Electrochim Acta 270: 453-460.

MATENCIO T, DE PAOLI MA, PERES RCD, TORRESI RM & CORDOBA DE TORRESI SI. 1995. Ionic exchanges in dodecylbenzenesulfonate doped polypyrrole Part 1. Optical beam deflection studies. Synth Met 72: 59-64.

MICHALCHUK AAL, TUMANOV IA & BOLDYREVA EV. 2013. Complexities of mechanochemistry: elucidation of processes occurring in mechanical activators via implementation of a simple organic system. CrystEngComm 15: 6403-6412.

MILLER JR & OUTLAW RA. 2015. Vertically-oriented graphene electric double layer capacitor designs. J Electrochem Soc 162: A5077-A5082.

MONDAL AK, SU D, CHEN S, KRETSCHMER K, XIE X, AHN HJ & WANG G. 2015. A microwave synthesis of mesoporous NiCo2O4 nanosheets as electrode materials for lithium-ion batteries and supercapacitors. ChemPhysChem 16: 169-175.

MONTEIRO MJ, BAZITO FFC, SIQUEIRA LJA, RIBEIRO MCC & TORRESI RM. 2008. Transport Coefficients, Raman Spectroscopy, and Computer Simulation of Lithium Salt Solutions in an Ionic Liquid. J Phys Chem B 112: 2102-2109.

MONTEIRO MJ, CAMILO FF, RIBEIRO MCC & TORRESI RM. 2010. Ether-Bond-Containing Ionic Liquids and the Relevance of the Ether Bond Position to Transport Properties. J Phys Chem B 114: 12488-12494.

MOTTILLO C & FRIŠČIĆ T. 2017. Advances in Solid-State Transformations of Coordination Bonds: From the Ball Mill to the Aging Chamber. Molecules 22: 144.

MUÑOZ-BATISTA MJ, RODRIGUEZ-PADRON D, PUENTE-SANTIAGO AR & LUQUE R. 2018. Mechanochemistry: Toward Sustainable Design of Advanced Nanomaterials for Electrochemical Energy Storage and Catalytic Applications. ACS Sustain Chem Eng 6: 9530-9544.

MURALIGANTH T, VADIVEL MURUGAN A & MANTHIRAM A. 2009. Facile synthesis of carbon-decorated single-crystalline Fe3 O4 nanowires and their application as high performance anode in lithium ion batteries. Chem Commun 7360-7362.

MUZAFFAR A, AHAMED MB, DESHMUKH K & THIRUMALAI J. 2019. A review on recent advances in hybrid supercapacitors: Design, fabrication and applications. Renew Sustain Energy Rev 101: 123-145.

NAGUIB M, KURTOGLU M, PRESSER V, LU J, NIU J, HEON M, HULTMAN L, GOGOTSI Y & BARSOUM MW. 2011. Two-dimensional nanocrystals produced by exfoliation of Ti 3AlC 2. Adv Mater 23: 4248-4253.

NAGUIB M, MASHTALIR O, CARLE J, PRESSER V, LU J, HULTMAN L, GOGOTSI Y & BARSOUM MW. 2012. Two-dimensional transition metal carbides. ACS Nano 6: 1322-1331.

NAMBU N, TAKAHASHI R, SUZUKI K & SASAKI Y. 2013. Electrolytic properties of tetramethylammonium compound in highly concentrated solutions and its application to electric double-layer capacitors. Electrochemistry 81: 811-813.

NANBU N, EBINA T, UNO H, MIYAZAKI Y & SASAKI Y. 2006a. Thermal and Electrolytic Properties of Quaternary Ammonium Salts Based on Fluorine-Free Chelatoborate Anions and Their Application to EDLCs. Electrochem Solid-State Lett 9: A482.

NANBU N, EBINA T, UNO H, ISHIZAWA S & SASAKI Y. 2006b. Physical and electrochemical properties of quaternary ammonium bis(oxalato)borates and their application to electric double-layer capacitors. Electrochim Acta 52: 1763-1770.

NANBU N, SUZUKI K, EBINA T, UNO H & SASAKI Y. 2007. Tetramethylammonium Difluoro(oxalato)borate as Novel Electrolyte for Electric Double-Layer Capacitors. Electrochemistry 75: 615-618.

NETO DBF, XAVIER FFS, MATSUBARA EY, PARMAR R, GUNNELLA R & ROSOLEN JM. 2020. The role of nanoparticle concentration and CNT coating in high-performance polymer-free micro/nanostructured carbon nanotube-nanoparticle composite electrode for Li intercalation. J Electroanal Chem 858: 113826.

NEVES S & POLO FONSECA C. 2002. Influence of template synthesis on the performance of polyaniline cathodes. J Power Sources 107: 13-17.

NICOLOSI V, CHHOWALLA M, KANATZIDIS MG, STRANO MS & COLEMAN JN. 2013. Liquid Exfoliation of Layered Materials. Science 340: 1226419.

NING LJ, WU YP, FANG SB, RAHM E & HOLZE R. 2004. Materials prepared for lithium ion batteries by mechanochemical methods. J Power Sources 133: 229-242.

OHZUKU T, SAWAI K & HIRAI T. 1987. Electrochemistry of L-niobium pentoxide a lithium/non-aqueous cell. J Power Sources 19: 287-299.

OKUBO M, HOSONO E, KIM J, ENOMOTO M, KOJIMA N, KUDO T, ZHOU H & HONMA I. 2007. Nanosize Effect on High-Rate Li-Ion Intercalation in LiCoO2 Electrode. J Am Chem Soc 129: 7444-7452.

OLIVEIRA PFM, WILLART JF, SIEPMANN J, SIEPMANN F & DESCAMPS M. 2018. Using Milling To Explore Physical States: The Amorphous and Polymorphic Forms of Dexamethasone. Cryst Growth Des 18: 1748-1757.

PAN Y, LIU Y, ZENG G, ZHAO L & LAI Z. 2011. Rapid synthesis of zeolitic imidazolate framework-8 (ZIF-8) nanocrystals in an aqueous system. Chem Commun 47: 2071.

PATAKE VD, LOKHANDE CD & JOO OS. 2009. Electrodeposited ruthenium oxide thin films for supercapacitor: Effect of surface treatments. Appl Surf Sci 255: 4192-4196.

PECHINI MP. 1967 Method of preparing lead and alkaline earth titanates and niobates and coating method using the same to form a capacitor. United States Patent Office. 3,330,697.

PENG YY ET AL. 2016. All-MXene (2D titanium carbide) solid-state microsupercapacitors for on-chip energy storage. Energy Environ Sci 9: 2847-2854.

PERES RCDD, DE PAOLI MA & TORRESI RM. 1992. The role of ion exchange in the redox processes of polypyrrole/dodecyl sulfate films as studied by electrogravimetry using a quartz crystal microbalance. Synth Met 48: 259-270.

POHLMANN S, OLYSCHLÄGER T, GOODRICH P, ALVAREZ VICENTE J, JACQUEMIN J & BALDUCCI A. 2015. Azepanium-based ionic liquids as green electrolytes for high voltage supercapacitors. J Power Sources 273: 931-936.

PONT AL, MARCILLA R, DE MEATZA I, GRANDE H & MECERREYES D. 2009. Pyrrolidinium-based polymeric ionic liquids as mechanically and electrochemically stable polymer electrolytes. J Power Sources 188: 558-563.

QIN Z, ZHOU X, XIA Y, TANG C & LIU Z. 2012. Morphology controlled synthesis and modification of high-performance LiMnPO4 cathode materials for Li-ion batteries. J Mater Chem 22: 21144-21153.

RAGUPATHI V, PANIGRAHI P & NAGARAJAN GS. 2019. Enhanced electrochemical performance of nanopyramid-like LiMnPO4/C cathode for lithium-ion batteries. Appl Surf Sci 495: 143541.

RAMACHANDRAN R & WANG F. 2018. Electrochemical Capacitor Performance: Influence of Aqueous Electrolytes. In: Supercapacitors - Theor Pract Solut InTech, p. 51-68.

RENNIE AJR, MARTINS VL, TORRESI RM & HALL PJ. 2015. Ionic Liquids Containing Sulfonium Cations as Electrolytes for Electrochemical Double Layer Capacitors. J Phys Chem C 119: 23865-23874.

RENNIE AJR, SANCHEZ-RAMIREZ N, TORRESI RM & HALL PJ. 2013. Ether-Bond-Containing Ionic Liquids as Supercapacitor Electrolytes. J Phys Chem Lett 4: 2970-2974.

RYU KS, KIM KM, PARK NG, PARK YJ & CHANG SH. 2002. Symmetric redox supercapacitor with conducting polyaniline electrodes. J Power Sources 103: 305-309.

SALANNE M. 2017. Ionic Liquids for Supercapacitor Applications. Top Curr Chem 375: 63.

SALVATIERRA RV, DOMINGUES SH, OLIVEIRA MM & ZARBIN AJG. 2013. Tri-layer graphene films produced by mechanochemical exfoliation of graphite. Carbon 57: 410-415.

SANG X, XIE Y, LIN MW, ALHABEB M, VAN AKEN KL, GOGOTSI Y, KENT PRC, XIAO K & UNOCIC RR. 2016. Atomic Defects in Monolayer Titanium Carbide (Ti3C2Tx) MXene. ACS Nano 10: 9193-9200.

SCHÜTTER C, HUSCH T, KORTH M & BALDUCCI A. 2015. Toward New Solvents for EDLCs: From Computational Screening to Electrochemical Validation. J Phys Chem C 119: 13413-13424.

SCHÜTTER C, HUSCH T, VISWANATHAN V, PASSERINI S, BALDUCCI A & KORTH M. 2016. Rational design of new electrolyte materials for electrochemical double layer capacitors. J Power Sources 326: 541-548.

SHI W, SONG S & ZHANG H. 2013. Hydrothermal synthetic strategies of inorganic semiconducting nanostructures. Chem Soc Rev 42: 5714-5743.

SHI Y, PENG L & YU G. 2015. Nanostructured conducting polymer hydrogels for. Nanoscale 7: 12796-12806.

SILLARS FB, FLETCHER SI, MIRZAEIAN M & HALL PJ. 2011. Effect of activated carbon xerogel pore size on the capacitance performance of ionic liquid electrolytes. Energy Environ Sci 4: 695-706.

SIMERAL L & AMEY RL. 1970. Dielectric properties of liquid propylene carbonate. J Phys Chem 74: 1443-1446.

SIMON P & GOGOTSI Y. 2008. Materials for electrochemical capacitors. Nat Mater 7: 845-854.

SNOOK GA, CHEN GZ, FRAY DJ, HUGHES M & SHAFFER M. 2004. Studies of deposition of and charge storage in polypyrrole-chloride and polypyrrole-carbon nanotube composites with an electrochemical quartz crystal microbalance. J Electroanal Chem 568: 135-142.

SNOOK GA, KAO P & BEST AS. 2011. Conducting-polymer-based supercapacitor devices and electrodes. J Power Sources 196: 1-12.

SOIRON S, ROUGIER A, AYMARD L & TARASCON JM. 2001. Mechanochemical synthesis of Li-Mn-O spinels: positive electrode for lithium batteries. J Power Sources 97-98: 402-405.

SOUDAN P, LUCAS P, HOANG AH, JOBIN D, BREAU L & BÉLANGER D. 2001. Synthesis, chemical polymerization and electrochemical properties of low band gap conducting polymers for use in supercapacitors. J Mater Chem 11: 773-782.

SURYANARAYANA C. 2001. Mechanical alloying and milling. Prog Mater Sci 46: 1-184.

TANG Y ET AL. 2014. Unravelling the correlation between the aspect ratio of nanotubular structures and their electrochemical performance to achieve high-rate and long-life lithium-ion batteries. Angew Chemie - Int Ed 53: 13488-13492.

TARASCON JM, MORCRETTE M, SAINT J, AYMARD L & JANOT R. 2005. On the benefits of ball milling within the field of rechargeable Li-based batteries. Comptes Rendus Chim 8: 17-26.

THACKERAY MM, JOHNSON PJ, DE PICCIOTTO LA, BRUCE PG & GOODENOUGH, JB. 1984. Electrochemical extraction of lithium from LiMn2O4. Mater Res Bull 19: 179-187.

TITIRICI MM, WHITE RJ, BRUN N, BUDARIN VL, SU DS, DEL MONTE F, CLARK, JH & MACLACHLAN MJ. 2015. Sustainable carbon materials. Chem Soc Rev 44: 250-290.

TOLOSA A, KRÜNER B, FLEISCHMANN S, JÄCKEL N, ZEIGER M, ASLAN M, GROBELSEK I & PRESSER V. 2016. Niobium carbide nanofibers as a versatile precursor for high power supercapacitor and high energy battery electrodes. J Mater Chem A 4: 16003-16016.

TORRESI RM, CÓRDOBA DE TORRESI SI, MATENCIO T & DE PAOLI MA. 1995. Ionic exchanges in dodecylbenzenesulfonate-doped polypyrrole Part II: Electrochemical quartz crystal microbalance study. Synth Met 72: 283-287.

TORRESI RM, DE TORRESI, SIC, GABRIELLI C, KEDDAM M & TAKENOUTI H. 1993. Quartz crystal microbalance characterization of electrochemical doping of polyaniline films. Synth Met 61: 291-296.

TORRESI RM, CORRÊA CM, BENEDETTI TM & MARTINS VL. 2018. Tailoring Transport Properties Aiming for Versatile Ionic Liquids and Poly(Ionic Liquids) for Electrochromic and Gas Capture Applications. In: Polym Ion Liq Cambridge: Royal Society of Chemistry. 342-380.

TOUPIN M, BROUSSE T & BÉLANGER D. 2004. Charge Storage Mechanism of MnO 2 Electrode Used in Aqueous Electrochemical Capacitor. Chem Mater 16: 3184-3190.

TREWYN BG, SLOWING II, GIRI S, CHEN HT & LIN VSY. 2007. Synthesis and Functionalization of a Mesoporous Silica Nanoparticle Based on the Sol-Gel Process and Applications in Controlled Release. Acc Chem Res 40: 846-853.

VAN AKEN KL, BEIDAGHI M & GOGOTSI Y. 2015. Formulation of Ionic-Liquid Electrolyte To Expand the Voltage Window of Supercapacitors. Angew Chemie Int Ed 54: 4806-4809.

VARELA H, MALTA M & TORRESI RM. 2001. Microgravimetric study of the influence of the solvent on the redox properties of polypyrrole modified electrodes. J Power Sources 92: 50-55.

VERGER L, NATU V, CAREY M & BARSOUM MW. 2019a. MXenes: An Introduction of Their Synthesis, Select Properties, and Applications. Trends Chem 1: 656-669.

VERGER L, XU C, NATU V, CHENG HM, REN W & BARSOUM MW. 2019b. Overview of the synthesis of MXenes and other ultrathin 2D transition metal carbides and nitrides. Curr Opin Solid State Mater Sci 23: 149-163.

VILLERS D, JOBIN D, SOUCY C, COSSEMENT D, CHAHINE R, BREAU L & BÉLANGER D. 2003. The Influence of the Range of Electroactivity and Capacitance of Conducting Polymers on the Performance of Carbon Conducting Polymer Hybrid Supercapacitor. J Electrochem Soc 150: A747.

WANG GW. 2013. Mechanochemical organic synthesis. Chem Soc Rev 42: 7668-7700.

WANG G, ZHANG L & ZHANG J. 2012. A review of electrode materials for electrochemical supercapacitors. Chem Soc Rev 41: 797-828.

WANG J, XU Y, CHEN X & DU X. 2007. Electrochemical supercapacitor electrode material based on poly(3,4-ethylenedioxythiophene)/polypyrrole composite. J Power Sources 163: 1120-1125.

WANG L, ZHANG Y, SCOFIELD ME, YUE S, MCBEAN C, MARSCHILOK AC, TAKEUCHI KJ, TAKEUCHI ES & WONG SS. 2015a. Enhanced Performance of "flower-like" Li4Ti5O12 Motifs as Anode Materials for High-Rate Lithium-Ion Batteries. ChemSusChem 8: 3304-3313.

WANG T, ZHAI Y, ZHU Y, LI C & ZENG G. 2018. A review of the hydrothermal carbonization of biomass waste for hydrochar formation: Process conditions, fundamentals, and physicochemical properties. Renew Sustain Energy Rev 90: 223-247.

WANG X, YAN C, YAN J, SUMBOJA A & LEE PS. 2015b. Orthorhombic niobium oxide nanowires for next generation hybrid supercapacitor device. Nano Energy 11: 765-772.

WEI C, SHEN J, ZHANG J, ZHANG H & ZHU C. 2014. Effects of ball milling on the crystal face of spinel LiMn 2 O 4. RSC Adv 4: 44525-44528.

WEINGARTH D, NOH H, FOELSKE-SCHMITZ A, WOKAUN A & KÖTZ R. 2013. A reliable determination method of stability limits for electrochemical double layer capacitors. Electrochim Acta 103: 119-124.

WOLFF C, JEONG S, PAILLARD E, BALDUCCI A & PASSERINI S. 2015. High power, solvent-free electrochemical double layer capacitors based on pyrrolidinium dicyanamide ionic liquids. J Power Sources 293: 65-70.

WU L, BUCHHOLZ D, VAALMA C, GIFFIN GA & PASSERINI S. 2016. Apple-Biowaste-Derived Hard Carbon as a Powerful Anode Material for Na-Ion Batteries. ChemElectroChem 3: 292-298.

WU XL, WEN T, GUO HL, YANG S, WANG X & XU AW. 2013. Biomass-Derived Sponge-like Carbonaceous Hydrogels and Aerogels for Supercapacitors. ACS Nano 7: 3589-3597.

XIA Q, NI M, CHEN M & XIA H. 2019. Low-temperature synthesized self-supported single-crystalline LiCoO2 nanoflake arrays as advanced 3D cathodes for flexible lithium-ion batteries. J Mater Chem A 7: 6187-6196.

XUE Z, HE D & XIE X. 2015. Poly(ethylene oxide)-based electrolytes for lithium-ion batteries. J Mater Chem A 3: 19218-19253.

YAMADA A, CHUNG SC & HINOKUMA K. 2001. Optimized LiFePO4 for Lithium Battery Cathodes. J Electrochem Soc 148: A224.

YANG LC, QU QT, SHI Y, WU YP & VAN REE T. 2010 Materials for lithium-ion batteries by mechanochemical methods. In: High-Energy Ball Milling. Woodhead Publishing, p. 361-408.

YANG Z, CHOI D, KERISIT S, ROSSO KM, WANG D, ZHANG J, GRAFF G & LIU J. 2009. Nanostructures and lithium electrochemical reactivity of lithium titanites and titanium oxides: A review. J Power Sources 192: 588-598.

YAO L, DENG H, HUANG QA, SU Q & DU G. 2017. Three-dimensional carbon-coated ZnFe2O4 nanospheres/nitrogen-doped graphene aerogels as anode for lithium-ion batteries. Ceram Int 43: 1022-1028.

YOON S & MANTHIRAM A. 2011. Microwave-hydrothermal synthesis of W0.4Mo0.6O 3 and carbon-decorated WOx-MoO2 nanorod anodes for lithium ion batteries. J Mater Chem 21: 4082-4085.

YUAN C, LI J, HOU L, LIN J, PANG G, ZHANG L, LIAN L & ZHANG X. 2013. Template-engaged synthesis of uniform mesoporous hollow NiCo 2O4 sub-microspheres towards high-performance electrochemical capacitors. RSC Adv 3: 18573-18578.

YU L, ZHANG G, YUAN C & LOU XW. 2013. Hierarchical NiCo2O4@MnO2 core-shell heterostructured nanowire arrays on Ni foam as high-performance supercapacitor electrodes. Chem Commun 49: 137-139.

ZHANG X, HOU L, CIESIELSKI A & SAMORÌ P. 2016. 2D Materials Beyond Graphene for High-Performance Energy Storage Applications. Adv Energy Mater 6: 1600671.

ZHANG X, ZHANG H, LI C, WANG K, SUN X & MA Y. 2014. Recent advances in porous graphene materials for supercapacitor applications. RSC Adv 4: 45862-45884.

ZHAO X, HOU Y, WANG Y, YANG L, ZHU L, CAO R, SHA Z. 2017. Prepared MnO2 with different crystal forms as electrode materials for supercapacitors: experimental research from hydrothermal crystallization process to electrochemical performances. RSC Adv 7: 40286-40294.

ZHONG XB, YANG ZZ, WANG HY, LU L, JIN B, ZHA M, JIANG QC. 2016. A novel approach to facilely synthesize mesoporous ZnFe2O4 nanorods for lithium ion batteries. J Power Sources 306: 718-723.

ZHOU G, XU L, HU G, MAI L, CUI Y. 2019a. Nanowires for Electrochemical Energy Storage. Chem Rev 119: 11042-11109.

ZHOU S, TAO Z, LIU J, WANG X, MEI T, WANG X. 2019b. Bricklike Ca9Co12O28 as an Active/Inactive Composite for Lithium-Ion Batteries with Enhanced Rate Performances. ACS Omega 4: 6452-6458.

How to cite
MARTINS VL ET AL. 2020. An Overview on the Development of Electrochemical Capacitors and Batteries – Part I. An Acad Bras Cienc 92: e20200796. DOI 10.1590/0001-3765202020200796.

Manuscript received on May 23, 2020;
accepted for publication on May 25, 2020

VITOR L. MARTINS[1]
https://orcid.org/0000-0002-8824-7328

HERBERT R. NEVES[1,2]
https://orcid.org/0000-0001-7756-5278

IVONNE E. MONJE[1]
https://orcid.org/0000-0002-1220-3580

MARINA M. LEITE[1]
https://orcid.org/0000-0002-4569-5673

PAULO F.M. DE OLIVEIRA[1]
https://orcid.org/0000-0003-4854-5352

RODOLFO M. ANTONIASSI[1]
https://orcid.org/0000-0002-7027-7860

SUSANA CHAUQUE[1]
https://orcid.org/0000-0003-3950-6538

WILLIAM G. MORAIS[1]
https://orcid.org/0000-0001-6686-8687

EDUARDO C. MELO[1]
https://orcid.org/0000-0002-3489-9865

THIAGO T. OBANA[1]
https://orcid.org/0000-0002-0644-9883

BRENO L. SOUZA[1]
https://orcid.org/0000-0001-6774-2664

ROBERTO M. TORRESI[1]
https://orcid.org/0000-0003-4414-5431

[1]Universidade de São Paulo, Depto. Química Fundamental, Instituto de Química, Av. Prof. Lineu Prestes, 748, 05508-000 São Paulo, SP, Brazil

[2]Catarinense Federal Institute for Education Science and Technology – IFC, Campus Araquari, Rodovia BR280, Km 27, s/n, C.P. 21, 89245-000 Araquari, SC, Brazil

Correspondence to: **Roberto Manuel Torresi**
E-mail: rtorresi@iq.usp.br

Author contributions

VLM: Conceptualization, Writing original draft preparation and Writing-Reviewing and Editing. HRN, IEM, PMO, RMA, SC, WGM, EC, TTO, BLS: Writing original draft preparation. MML: Writing original draft preparation and Reviewing last version. RMT: Conceptualization, Supervision, Writing-Reviewing last version.